CARBON DIOXIDE (CO_2) REFORMING OF METHANE TO SYNGAS OVER NI/SBA-15 CATALYST

MOHAMAD IRSYAD BIN OTHMAN

BACHELOR OF CHEMICAL ENGINEERING

UNIVERSITI MALAYSIA PAHANG

Thesis Access Form

No_____Location_____

Author : ……

Title : ……

Status of access OPEN / RESTRICTED / CONFIDENTIAL

Moratorium period:_____ years, ending_____/_____200____

Conditions of access proved by (CAPITALS): DR. NURUL AINI BINTI MOHAMED RAZALI
Supervisor (Signature)……

Faculty: ……

Author's Declaration: *I agree the following conditions:*

OPEN access work shall be made available in the Universiti Malaysia Pahang only and not allowed to reproduce for any purposes.

*The statement itself shall apply to **ALL** copies:*

This copy has been supplied on the understanding that it is copyright material and that no quotation from the thesis may be published without proper acknowledgement.

Restricted/confidential work: All access and any photocopying shall be strictly subject to written permission from the University Head of Department and any external sponsor, if any.

Author's signature…….Date: ……

users declaration: for signature during any Moratorium period (Not Open work): ***I undertake to uphold the above conditions:***			
Date	Name (CAPITALS)	Signature	Address

CARBON DIOXIDE (CO_2) REFORMING OF METHANE TO SYNGAS OVER NI/SBA-15 CATALYST

MOHAMAD IRSYAD BIN OTHMAN

Thesis submitted in partial fulfilment of the requirements
for the award of the degree of
Bachelor of Chemical Engineering

Faculty of Chemical & Natural Resources Engineering

UNIVERSITI MALAYSIA PAHANG

DECEMBER 2014

SUPERVISOR'S DECLARATION

We hereby declare that we have checked this thesis and in our opinion, this thesis is adequate in terms of scope and quality for the award of the degree of Bachelor of Chemical Engineering.

Signature :
Name of main supervisor : DR. NURUL AINI BINTI MOHAMED RAZALI
Position : LECTURER
Date : 1st JULY 2015

STUDENT'S DECLARATION

I hereby declare that the work in this thesis is my own except for quotations and summaries which have been duly acknowledged. The thesis has not been accepted for any degree and is not concurrently submitted for award of other degree.

Signature :
Name : MOHAMAD IRSYAD BIN OTHMAN
ID Number : KA11076
Date : 1st JULY 2015

Dedication

To my family and my supervisor for their unlimited support with motivation, knowledge for making this research project successful. To my dearest friends which are my housemates, thank you so much that spend your times together. Gonna miss you guys.

ACKNOWLEDGEMENT

While this dissertation presents the research work carried out in my final years as a graduate student, it does not reflect the love, support, encouragement and guidance of many who have supported my journey here at University Malaysia Pahang and deserve more than just an acknowledgement. I am grateful for all the blessings given to me by Allah S.W.T for He is the One that make this all happen. I thank Him profusely for everything that He has given me, and pray that He continue to bless me in all my future endeavours.

I would like to specially acknowledge my honourable supervisor, Dr. Nurul Aini Binti Mohamed Razali for whom I have utmost respect and appreciation. This dissertation was possible mainly because of the opportunity given to be doing this research on this topic. Her lessons, dedication, enthusiasm, and passion for research motivated me to strive in completing this research work under her guidance. The support and encouragement she has given me during my years in University Malaysia Pahang will be remembered forever. Her philosophy and teaching style are unique, and will continue to impact me even after I graduate.

The journey through finishing this research would have been difficult without the company of my research mate: Muhammad Nazirul Bin Mok Hat. Thank you so much for your support and help during our period together.

Where I am today is because of my parents, and this dissertation is a reflection of the love and support that my parents have given me throughout my life. They have gone to great extents to make sacrifices for me and to ensure that all of my needs are met. I specially thank my father, Mr. Othman Bin Awang, who has made great strides to ensure that my brother, sister and I received the best possible education. He has inspired us to work hard in order to achieve our goals. I will be ever grateful to my parents for all the things they have done for us.

I would also like to acknowledge my mother, Mrs. Nurul Azian Binti Abu Kassim @ Mohd Kasim, who has motivated me to keep moving through difficult times. Her love and patience has been a tremendous source of strength for me during my years in University Malaysia Pahang. And last but not least, many thanks and appreciation to my dearest friends which are my housemates that spend your times since 2011. Your times, motivation, knowledge, and many things, I appreciate and I will remember this wonderful life as a university student’s. Thank you so much and I love u all.

ABSTRACT

Global emissions of carbon dioxide (CO_2) was the main cause of human-induced global warming which is increased by 1.1% at 34.5 billion tonnes in 2012. There are many ways to reduce CO_2 product such as conversion of CO_2 to fuel, utilization of CO_2 as a chemicals feedstock and non-conversion use of CO_2 utilization of CO_2 for methane reforming to syngas will be studied over Ni/SBA-15. The SBA-15 and Ni/SBA-15 will be synthesized by conversional and impregnation method, respectively. The chemical and physical characteristics of the catalysts before and after catalytic test will be investigated using X-ray diffraction (XRD), Thermogravimetric Analysis (TGA), Transmission Electron Microscope (TEM) and Brunauer–Emmett–Teller, Autosorb-1, Quantachrome (BET). SBA-15 have their unique structural features like high surface area, uniform and well defined pore topology. Nickel (Ni) based catalysts are one of the excellent catalyst systems for the CO_2 reforming to methane besides the noble metals catalysts. Ni/SBA-15 expected to exhibited excellent catalytic performance in terms of CO_2 conversion and long-term stability. The activity of the catalysts correlated strongly with the surface area and active site of the materials. This expectations was due to advantages of good structural stability and unique pore structural properties of SBA-15 as catalyst support and good active site of Ni, make this Ni/SBA-15 catalyst is suitable to be used for CO_2 reforming of methane. This expectation was due to the good structural stability and unique structural properties of SBA-15.

Keyword: *CO_2 reforming of methane, Synthesis gas, SBA-15, Ni/SBA-15, Hydrogen.*

ABSTRAK

Pelepasan secara besar-besaran gas karbon dioksida (CO_2) adalah punca utama pemanasan global. Hal ini disebabkan oleh populasi manusia yang meningkat sebanyak 1.1 % pada 34.5 bilion tan metrik untuk tahun 2012. Terdapat pelbagai kaedah untuk mengurangkan gas CO_2, antaranya adalah penukaran gas CO_2 kepada penjanaan, penggunaan gas CO_2 sebagai bahan mentah kimia dan penggunaan bukan-penukaran gas CO_2 dan pembaharuan gas CO2 untuk metana kepada syngas. Kaedah – kaedah ini akan dikaji melalui bahan Ni/SBA-15. SBA-15 dan Ni/SBA-15 yang akan disintesis menggunakan kaedah konversional dan impregnasi. Ciri-ciri kimia dan fizikal sebelum dan selepas ujian pemangkin akan disiasat menggunakan pembelauan sinar-X (XRD), Analisis Termogravimetri (TGA), Transmisi Elektron Mikroskop (TEM) dan Brunauer-Emmett-Teller, Autosorb-1, Quantachrome (BET). SBA-15 mempunyai ciri-ciri struktur yang unik seperti permukaan luas yang tinggi, seragam dan liang topologi yang baik. Nikel (Ni) yang berasaskan pemangkin adalah salah satu sistem pemangkin yang sangat baik untuk pembaharuan gas CO_2 kepada metana di samping pemangkin logam mulia. Ni/SBA-15 dijangka menunjukkan prestasi pemangkin yang sangat baik dari segi penukaran gas CO_2 dan kestabilan jangka panjang. Aktiviti pemangkin ini berkait rapat dengan kawasan permukaan dan permukaan yang aktif pada bahan tersebut. Jangkaan ini disebabkan oleh kelebihan kestabilan struktur yang baik dan sifat-sifat struktur liang yang unik pada SBA-15 sebagai pemangkin sokongan dan tapak aktif baik untuk Ni. Selain itu, Ni/SBA-15 juga menjadikan pemangkin ini sangat sesuai digunakan untuk pembaharuan gas CO_2 kepada metana disebabkan oleh kestabilan struktur yang baik dan sifat struktur yang unik SBA-15.

TABLE OF CONTENTS

SUPERVISOR'S DECLARATION IV
STUDENT'S DECLARATION V
Dedication VI
ACKNOWLEDGEMENT VII
ABSTRACT VIII
ABSTRAK IX
TABLE OF CONTENTS X
LIST OF FIGURES XII
LIST OF TABLES XIII
LIST OF ABBREVIATIONS XIV
1.0 INTRODUCTION
1.1 Background 1
1.2 Motivation and problem statement 2
1.3 Objective of Study 5
1.4 Scopes of Research 5
1.5 Main Contribution of This Work 5
1.6 Organisation of This Thesis 5
2.0 LITERATURE REVIEW
2.1 Greenhouse Gas Emission 7
2.2 CO_2 Reforming Of Methane 8
2.21 Syngas 9
2.22 Hydrogen (H_2) 11
2.23 Methane 11
2.3 Support Material 12
2.31 Silicon Dioxide (SiO_2) and Aluminium Oxide (Al_2O_3) 12
2.32 Metal Oxide 12
2.33 Nickel (Ni) 13
2.4 Santa Barbara Amorphous 15 (SBA-15) 15
2.5 Ni supported by SBA-15 (Ni/SBA-15) 18
3.0 MATERIALS AND METHODS
3.1 Overview 21
3.2 Methodology 21
3.21 Materials 21
3.22 Synthesis of catalyst 21
3.221 Synthesis of SBA-15 by conventional method 21

3.222 Synthesis of Ni/SBA-15 by impregnation method....22
3.23 Characterization of catalysts....22
3.24 Catalytic activity testing....22

4.0 RESULT AND DISCUSSION

4.1 Overview....24
4.2 Catalytic activity testing....24
4.3 Thermogravimetric analysis (TGA) testing....25
4.4 X-Ray diffraction (XRD) testing....26
4.5 Brunauer–Emmett–Teller, Autosorb-1, Quantachrome (BET) testing....27

5.0 CONCLUSION AND RECOMMENDATION

5.1 Conclusion....29
5.2 Recommendation....29

REFERENCES....30

APPENDICES....35

LIST OF FIGURES

Figure 1.1: Different pathways for utilizing CO_2 (Narasi & Davion, 2011). 2

Figure 1.2: Hydrogen consumption by region of production (Butterfield, 2013) 4

Figure 2.1: Existing bulk Carbon Dioxide (CO_2) market (Brinckerhoff, 2011) 9

Figure 2.2: Applications of syngas from Biomass/coal 10

Figure 2.3: High resolution transmission electron microscopy (HRTEM) micrographs of SBA-15 mesoporous silica. The size and morphology of the highly ordered hexagonal pores in a 2D array (a) with long 1D channels (b) (p6mm plane group) can be observed. 16

Figure 2.4: The effect of support on CH_4 (a) and CO_2 (b) conversion over Ni catalysts at 700°C and at GHSV of 52,000 mL $h^{-1}g^{-1}$. 19

Figure 3.1: Schematic diagram of the reactor set-up. 23

Figure 4.1: Graph of CH_4 conversion at 700^oC for 1, 3, and 5 wt% Ni content. 24

Figure 4.2: Graph of CO_2 conversion at 700^oC for 1, 3, and 5 wt% Ni content. 24

Figure 4.3: Graph yield of H_2 at 700^oC for 1, 3, and 5 wt% Ni content. 25

Figure 4.4: TGA graph of 1wt%, 3wt% and 5wt% Ni content. 26

Figure 4.5: XRD pattern of 1wt%, 3wt% and 5wt% Ni content. 27

LIST OF TABLES

Table 4.1: Structural and textural properties of SBA-15 and Ni-SBA-15 with different wt% of Ni content. 28

LIST OF ABBREVIATIONS

X	Conversion
F_{in}	Flowrate in
F_{out}	Flowrate out
Y	Yield
C_i	Composition for each component
C_s	Composition for standard GC
A_i	Area for each component
A_s	Area for standard GC

1.0 INTRODUCTION

1.1 Background

The CO_2 reforming of methane got attention from environmental and industrial perspective because conversion of greenhouse gases into synthesis gas with a low H_2/CO ratio using nickel based catalyst. Nickel based catalyst is highly active for the CO_2 reforming of methane, but it is easily deactivated due to coke formation and metal sintering during the reaction (Jin-Kwon, et al., 2007).

Various materials such as metal oxides, mixed metal oxides, and zeolite have been examined as supports to develop nickel based catalyst resistant due to coke formation. The most supports that always used was metal oxide which is in fine powder due to its large surface area. However, using fine powder as support has disadvantage on this application because its particles tend to agglomerate into large particles at high temperature.

Nowadays, several researchers have shown that mesoporous SBA-15 compound can be used as catalyst support with high metal loading and dispersion without destroying the SBA-15 support pore hexagonal structure. SBA-15 compound are more favorable to be apply as catalyst support because of its mesopores sizes of 46-300 Å and high surface area of ~800 m^2/g. Moreover, the recent discovery of ordered large-pore mesoporous SBA-15 compound with three dimensional mesoporous networks has extended the applications in catalysis and separation because it has the advantage in the diffusion and transportation of large molecules compared to one-dimensional mesopore structures (Jin-Kwon, et al., 2007).

This paper reports to investigate Ni/SBA-15 as catalyst for the CO_2 reforming of methane to syngas. SBA-15 compound had been synthesis by conventional method and nickel particles were loaded into SBA-15 (Ni/SBA-15) using impregnation method. The catalytic results obtained in this study were compared with those between previous researches related to this study.

1.2 Motivation and problem statement

Carbon Dioxide (CO_2) is a major greenhouse gas that affected the atmosphere since 1896 which is enhanced to global warming. CO_2 in atmosphere can make a major effect of hurricanes (Knutson, et al., 1998), influence of El Nino phenomena (Feely, et al., 1999), reduce calcification of marines life (Barker & Elderfield, 2002; Riebesell, et al., 2000), and deglaciation (Montanez, et al., 2007). Therefore, the accumulation of CO_2 in atmosphere become a serious issues that need to be solved for environmental aspect.

The CO_2 emission involved fossil fuels when it burned from power plants comes from fuel combustion activities, industrial processes and natural gas processing, oil refineries, large industrial facilities and a few daily activities. The other types of CO_2 emitted from industrial production processes that can transform materials chemically, physically or biologically was uses of fuels as feedstocks in petrochemical processes (Chauvel & Lefebvre, 1989; Christensen & Primdahl, 1994).

From the Figure 1, CO_2 can be utilized in three major pathways which are as a storage medium for renewable energy, as a feedstock for various chemicals, and as a solvent or working fluid (Narasi & Davion, 2011). The uses of CO_2 to convert into various renewable fuels now widely supported by industry and governments because it can secure the future energy supplies and in order to decrease CO_2 emissions to atmosphere.

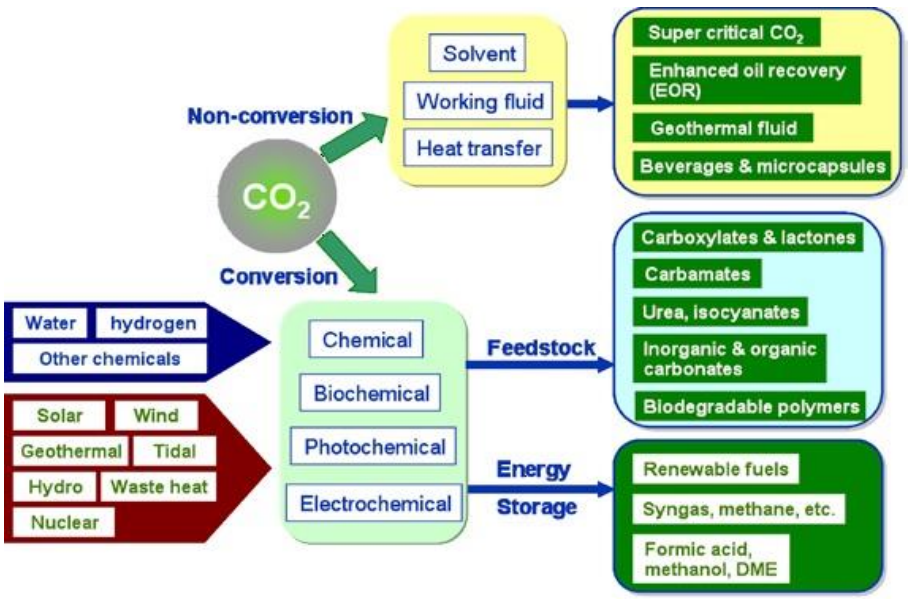

Figure 1.1: Different pathways for utilizing CO_2 (Narasi & Davion, 2011).

CO_2 can also be utilized as a part of different processes without convert it into other chemical structures. The injection of supercritical CO_2 into exhausted oil wells to improve the further recovery of oil is entrenched. In fact, this is in no time the main monetarily practical innovation for carbon capture and storage (CCS). It has been evaluated that CO_2 injection can build oil recovery from a well-draining by around 10 to 20 % of the first oil set up. Additionally, CO_2 can be utilized to recover methane from unmined coal creases. It has been estimated that in the U.S. alone, 89 billion barrels of oil could be recovered using CO_2, prompting a stockpiling of 16 Gt of CO_2 in the drained oil reservoirs (Shailesh, et al., 2013).

In addition, to produce biomass, chemical and electrochemical processes have been converted from CO_2 to other energy storage chemicals such as syngas, formic acid, methane, ethylene, methanol, and dimethyl ether (Olah, et al., 2009). Although it is more productive to utilize the electrical energy derived from renewable power sources straightforwardly, their variability represents an issue for many industries. Besides, the circulation base for hydrocarbon fuel is settled. At last, chemicals, for example, formic acid may be a valuable storage medium for H_2 that could be utilized as a part of energy components or blazed specifically (Narasi & Davion, 2011).

The hydrogen (H_2) market offers an energy for the future world that claimed as clean, safe and multifunction fuel. Production of H_2 can be produced from a chemical processes through a fossil fuel, biomass conversion, electrolytic, biophotololytic, or thermochemical splitting of water. H_2 can stores chemically or physically and converts to electrical and heat energy for the other uses. The biological world began developing H_2 market three billion years ago using H_2, C, and O_2 to reduce the cycle of photosynthesis and respiration in order to secure the earth. The human-engineered H_2 economy can take similar advantages of H_2 from chemical and physical interactions with materials to adaptably link and variety of energy sources for multitude of energy uses (Butterfield, 2013).

In U.S., hydrogen is right now created 0.09 Mtons/yr on a production through steam reforming of natural gas. These days, the majority of the hydrogen originate from fossil fuels is utilized as a part of the manure, petroleum, and compound commercial enterprises. Common gas assets will be sufficient for a few decades to extend this ability to backing the Freedom CAR and Fuel Initiative. By 2030, it is expected that the utilization of hydrogen in fuel cell controlled vehicles and light trucks could supplant production of 18.3 MB everyday of

petroleum. Accepting that hydrogen controlled vehicles have 2.5 times the energy efficiency of enhanced fuel vehicles, this diminishment in petroleum utilization would require the annual production of pretty nearly 0.55 Mtons of hydrogen by 2030. On the off chance that the majority of this hydrogen were delivered by petroleum changing, the net funds in petroleum utilization would be 11 MB every day. The aggregate energy used for transportation, incorporates a significant segment of different sorts of vehicles that need represents a more challenging test to hydrogen generation (Butterfield, 2013).

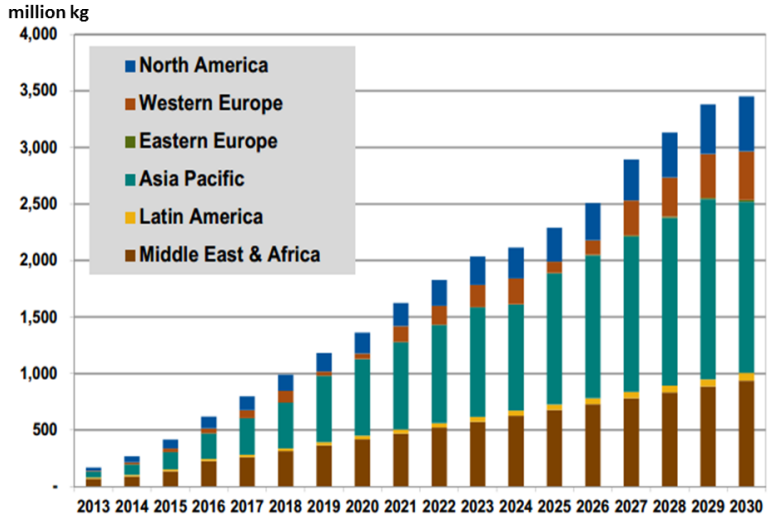

Figure 1.2: Hydrogen consumption by region of production (Butterfield, 2013)

There are many ways to reduce CO_2 and make it to useful product such as conversion of CO_2 to fuel using biomass, utilization of CO_2 as a chemicals feedstock, non-conversion use of CO_2 and also CO_2 reforming to syngas (Narasi & Davion, 2011). CO_2 reforming of methane, also known as dry reforming ($CH_{4(g)} + CO_{2(g)} \leftrightarrow 2CO_{(g)} + 2H_{2(g)}$) to syngas, which is can be used in various downstream chemical processes such as methanol production, Fischer-Tropsch synthesis processes and in carbonylation, hydrogenation, and hydroformylation processes (Amin, et al., 2012). In this work, CO_2 reforming of methane will be studied over Ni supported on mesoporous SBA-15 (Ni/SBA-15). This catalyst will be synthesized by conventional and impregnation method, respectively.

Due to previous research, SiO_2 and γ-Al_2O_3 have been the most often used for dry reforming of methane. Noble metal-supported catalysts (Rh, Ru, Pd, Pt, Ir) were founded to have promising catalytic performance in terms of conversion and selectivity for reforming of methane. But, because high cost of its make them not suitable choice for this process (Bradford

& Vannice, 1996; Fan, et al., 2009). Ni based catalyst is one of a good replacement for noble metals to be supported on SBA-15 because of higher activity, lower coke formation, and higher stability than Ni based catalysts supported on SiO_2 or γ -Al_2O_3 for the CO_2 reforming of methane (Jin-Kwon, et al., 2007).

1.3 Objective of Study

The objective of this study are to synthesis Ni/SBA-15 catalyst with suitable properties for CO_2 reforming of methane to syngas with high conversion and yield.

1.4 Scopes of Research

The scopes of this research are to mainly study about:

- To synthesis Ni/SBA-15 by using impregnation method with weight percentage of Ni loading (1, 3, 5 wt %).
- To characterize the catalyst properties by using X-ray diffraction (XRD), Thermogravimetric Analysis (TGA), Transmission Electron Microscope (TEM) and Brunauer–Emmett–Teller, Autosorb-1, Quantachrome (BET).
- To test catalyst performance via CO_2 reforming of methane to syngas.

1.5 Main Contribution of This Work

The following is the contribution:

- Prior to our supervisor's guidance in helping us learn and venture into Ni/SBA-15 on CO_2 reforming of methane to syngas.
- Be able to study the effects of weight percentage of Ni loading, characterization of catalyst and catalytic testing in CO_2 reforming of methane to syngas using fixed-bed reactor.

1.6 Organisation of This Thesis

The structure of the thesis is outlined as follow:

Chapter 1 described about the relationship between greenhouse gases that affected earth and CO_2 reforming of methane to syngas. Since H_2 can produce a lot of useful product that can reduce greenhouse gases produce in our daily life, it give a motivation to do a research about CO_2 reforming of methane to syngas using Ni/SBA-15. In this chapter also include scope, hypothesis and main contribution of this research.

Chapter 2 provides an overview of CO_2 reforming of methane using Ni/SBA-15 and Ni/SBA-15 synthesis by impregnation method. This chapter also provides a brief review on previous study on greenhouse gas emission, the best support material on SBA-15. A comparison that directly affect the performance between previous research and this research.

Chapter 3 described about the methodology involved in this research. The synthesis of SBA-15 and Ni/SBA-15 using conventional and impregnation method respectively, characterization of catalyst and catalytic activity testing for CO_2 reforming of methane.

Chapter 4 discussed on the effect of Ni loading with 1 wt%, 3 wt%, and 5 wt% on SBA-15 for CO_2 reforming of methane. The discussion on the reaction performance was related to the catalyst properties that obtained from XRD, BET, TGA, and TEM.

Chapter 5 draws together a summary of the thesis and outlines for the future work which might be derived from the experiment developed in this work.

2.0 LITERATURE REVIEW

2.1 Greenhouse Gas Emission

Svante Arrhenius (1859-1927) was a Swedish scientist that claim in 1896 that fossil fuel combustion may eventually result in enhanced global warming. He proposed a relation between atmospheric CO_2 concentrations and temperature. In the late 1950's and early 1960's, Charles Keeling used the newest technologies available to produce atmospheric CO_2 concentration curves in Antarctica and Mauna Loa. Therefore, fear began to develop that a new ice age might be near. The media and many scientists ignored scientific data of the 1950's and 1960's in favor of global cooling (Maslin, 2004; Enzler, 2014).

In 1940, there were advancements in infrared spectroscopy for measuring long-wave radiation. Around then it was demonstrated that increasing the amount of atmospheric carbon dioxide resulted in more absorption of infrared radiation. It was also discovered that water vapor consumed entirely unexpected sorts of radiation than CO_2. Gilbert Plass summarized these results in 1955. He concluded that adding more CO_2 to the air would catch infrared radiation that is generally lost to space, warming the earth.

Finally, in the 1980's, the global annual mean temperature curve started to rise. In the late 1980's, the curve began to increase so steeply that the global warming theory began a hot news topic that was repeated on a global scale. A complete media circus evolved that convinced many people we are on the edge of a significant climate change that has many negative impacts on our world today. Stephen Schneider was an experts about world's leading global warming that had a first predicted of global warming in 1976 (Maslin, 2004; Enzler, 2014).

In the 1990's scientists started to question the greenhouse effect theory, because of major uncertainties in the data sets and model outcomes. In 1998, it was globally the warmest year on record, followed by 2001, 2002, 2003 and 1997. The 10 warmest years on record have all occurred since 1990. So far not many measures have been taken to do something about climate change. This is largely caused by the major uncertainties still in the theory. Therefore in 1998 the Kyoto Protocol was negotiated in Kyoto, Japan and it requires participating countries to reduce their anthropogenic greenhouse gas emissions (CO_2, CH_4, N_2O, HFCs,

PFCs, and SF_6) by at least 5% below 1990 levels in the commitment period 2008 to 2012 (Maslin, 2004; Enzler, 2014).

Environmental change made by anthropogenic greenhouse gases has created the most basic biological issues standing up to the all-inclusive gathering. The supporters of the Protocol applauded it as a jump forward in overall air approach, in light of the fact that it secured an extensive worldwide framework for extending and creating climate security practices later on. Foes to the Protocol rejected it as a "significantly blemished comprehension that makes sense of how to be both fiscally inefficient and politically strange" (McKibbin & Wilcoxen, 2002).

Actually, after years of dull transactions on its solid execution, the Protocol has yet to go into energy, sitting tight for Russia to interpret its certain open reports into lawful sanction. Additionally, the U.S. refusal to approve the Protocol and the full tradability of discharge privileges surrendered to the previous Eastern Bloc in overabundance of its foreseen future the same old thing discharges (supposed hot air) infer that the present round of the Kyoto Protocol is liable to fulfill almost no regarding worldwide emanation decreases (Buchner, et al., 2002). This development appears to affirm the position of the Protocol's adversaries that its key methodology – setting targets and timetables for discharge decreases - is truly imperfect. Against this foundation, I need to give a discriminating evaluation of the Protocol's expected execution and examine potential changes to encourage adequacy and productivity in ensuing duty period (Böhringer, 2002).

2.2 CO_2 Reforming Of Methane

As the way to reduce CO_2 gas that affect the atmosphere, previous researchers have done invention such as in food industry they use it in food processing, preservation, food packaging, beverage carbonation, coffee decaffeination, and wine making. In other industry, CO_2 was used it to enhance oil recovery, urea fertiliser production, water treatment, steel manufacture, metal working, pulp and paper processing, and many of it that used in our life. Furthermore, CO_2 was used to make the medicine in pharmaceutical sector. From the further research, CO_2 can convert to various useful things such as liquid fuel, electricity and synthesis gas (syngas) as shown in Figure 3 (Brinckerhoff, 2011).

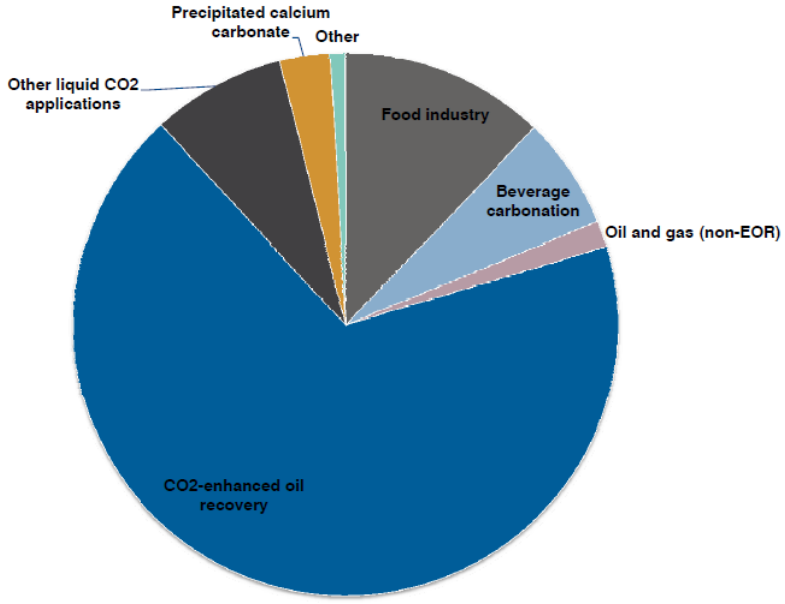

Figure 2.1: Existing bulk Carbon Dioxide (CO_2) market (Brinckerhoff, 2011)

2.21 Syngas

Synthesis gas or syngas can be produced from different materials that contain carbon. These can include in biomass, plastics, coal, municipal waste or similar materials. Syngas can produced from gasification or pyrolysis of carbonaceous materials. Gasification can be involved these subjecting materials to high temperatures, in controlled presence of oxygen with limited combustion to provide thermal energy to sustain the reaction. Man-made vessels, or alternatively could be conducted in-situ can be occurred in the gas of underground coal gasification. There are two types of gasifier. One of it is fuel to the gasifier where it is a recent biological origin, such as wood or organic waste, the gas produced by the gasifier is considered to be renewable and that is the power produced by the combustion. Second is fuel to the gasifier where it is a waste stream, the conversion to power in this manner has the combined benefit of the conversion of this waste into useful products. Generation of renewable power, conversion of problematic wastes to useful fuels, economical onsite power production and reduced transmission losses and reduction in carbon emissions are the benefits of synthesis gas. From the Figure 4, there are many useful product can produce from syngas and also can reduce the emission that affected the atmosphere (Bhd., n.d.)

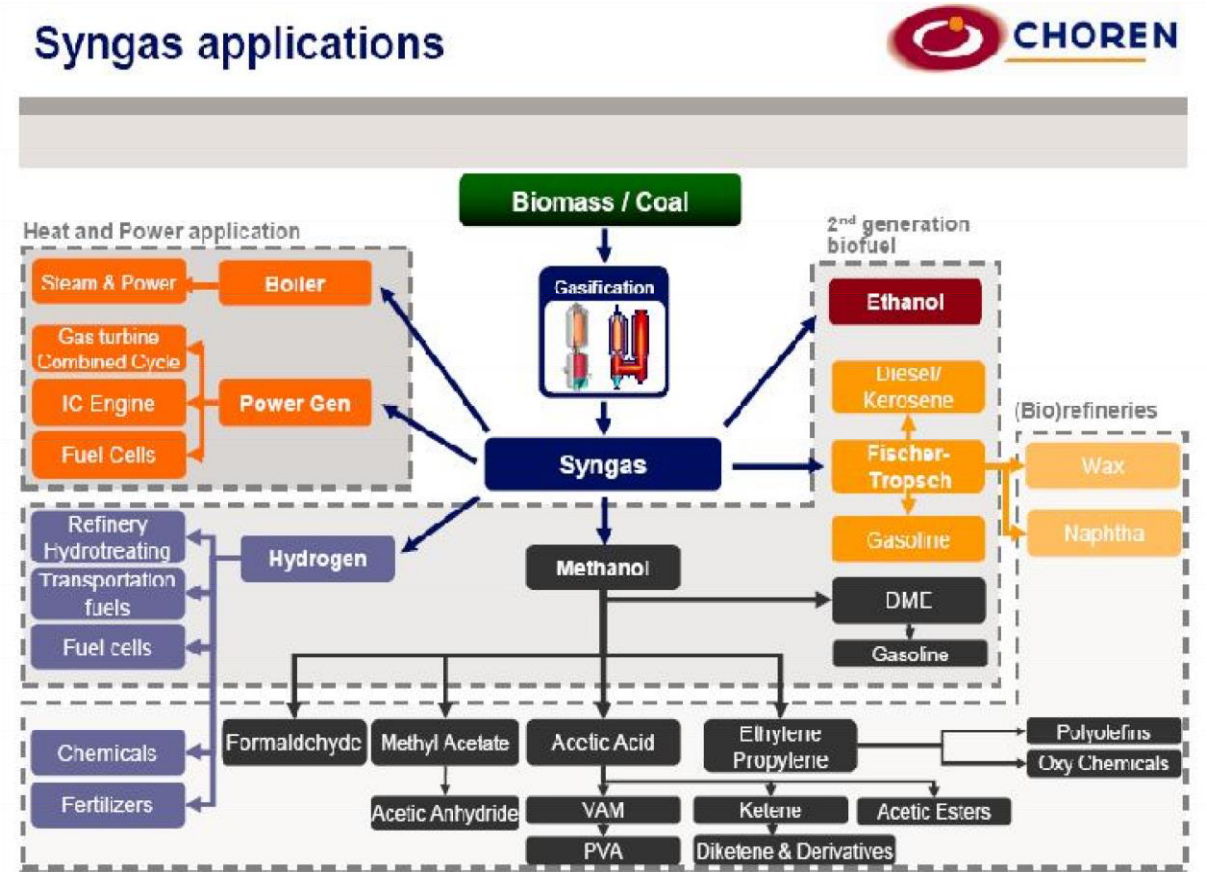

Figure 2.2: Applications of syngas from Biomass/coal

These last issues have animated examination into the development of synthesis gas by the carbon dioxide reforming of methane (dry reforming). The carbon dioxide reforming of methane, indeed, has been of enthusiasm for quite a while, going back to as right on time as the 1920's (Fischer & Tropsch, 1928), however it is just as of late that enthusiasm for it has quickly expanded for both ecological and business reasons. This reaction can performed as:

$$CH_4 + CO_2 \rightarrow 2CO + 2H_2 \qquad (1)$$

This procedure has numerous attractive preferences over dry reforming: (i) Synthesis gas has a CO/CO_2 ratio without further, post-reformer reaction. (ii) The utilization of CO_2 implies that it is an appealing course toward CO_2 relief in stationary anthropogenic sources. (iii) It permits the conversion of methane, beforehand a waste part of oil stores, into a financially alluring feedstock (Zhang, et al., 2003).

2.22 Hydrogen (H_2)

Other settled carbon stores, for example, coal or biomass feedstocks, could be utilized to create hydrogen through reforming methods. With respect to natural gas, these assets create more or less twice as much CO_2 every amount of hydrogen produced. This element puts extra weight on the advancement and economics of carbon sequestration. These feedstocks additionally contain variable measures of water, sulfur, nitrogen, and nonvolatile minerals that considerably convolute reforming process engineering. By and by, if a monetary and safe system for CO_2 sequestration is created, financial elements (the general accessibility and generally minimal effort of coal) may empower coal to play a noteworthy mid-term part in hydrogen era. Dependence on coal as a sole wellspring of vitality for producing hydrogen for Freedom CAR transportation needs would oblige multiplying of current local coal generation and utilization. Two effective methods for hydrogen production from coal or biomass are being worked on: (i) reforming under partial oxidation and (ii) a joined cycle strategy that uses $Ca(OH)_2$ to constrain the reforming reaction by adsorbing CO_2 as it is produced (Lin, et al., 2002).

In spite of the fact that the innovation is accessible for creating hydrogen in amount through reforming of natural gas or potentially other carbon holds, the hydrogen produced is not of sufficient purity for immediate use in the low-temperature (<130°C) fuel cells being worked on for transportation applications. The last stage in current reforming processes, the water-gas shift reaction, leaves enough carbon monoxide (CO) in the product stream to toxin the fuel cell anode. Current strategies for evacuating this leftover CO incorporate pressure-swing adsorption, particular oxidation, or catalytic methanation, all of which add expense and multifaceted nature to the fuel handling framework. Essential examination can supply elective answers for this issue, which could come as more active catalysts for the low-temperature water-gas shift reaction, better gas stream separation processes and membranes, or CO-tolerant catalysts at the fuel cell anode (Lin, et al., 2002).

2.23 Methane

Since methane was discovered to be a dominating segment of regular gas, late studies on the usage of natural gas have been focused only on catalytic conversion of methane to syngas. As characteristic gas is found in numerous areas around the globe, the catalytic conversion of methane would create syngas which is a crude material for some mechanical

items, for example, manures, explosives, chloroform and carbon tetrachloride. Syngas is additionally a vital source of methanol. The procedure of POM (partial oxidation of methane) shows gentle exothermicity. Contrasted with steam reforming, the catalytic partial oxidation is assessed to offer vitality cost decrease of around 30% since the response is exothermic. An included favorable position is that the syngas created has the CO/CO_2 molar ratio of around 2 and this makes the POM process perfect for the creation of amalgamation gas for utilization in methanol or Fischer-Tropsch synthesis (Habimana, et al., 2009).

2.3 Support Material

2.31 Silicon Dioxide (SiO_2) and Aluminium Oxide (Al_2O_3)

A few decade ago, the research on CO_2 reforming of methane has been developed of improved materials using catalytic reaction. Different types of catalysts have been used for dry reforming but from an industrial perspective, Ni based catalysts was the most often catalysts for dry reforming of methane. This reactions are considered the most promising which is exhibit high catalytic activity (Ferreira-Aparicio, et al., 1998), are readily available, and cost effective.

Since 1979 (Sodesawa, et al., 1979) and 1980 (Chubb, 1980), Ni/SiO_2 and Ni/Al_2O_3 have been the most often used catalysts for dry reforming of methane. This interest has been mostly due to SiO_2 and γ-Al_2O_3 with melting points of 1973°C and 2318°C (Richardson, 1989) having high mechanical strength and relatively low cost. Although noble metal-supported catalysts (Co, Ni, Ru, Rh, Pd and Pt. La and Zr) were founded to have promising catalytic performance in terms of conversion and selectivity for reforming of methane, the high cost of noble metals makes them a less than ideal choice (Bradford & Vannice, 1999; Fan, et al., 2009).

2.32 Metal Oxide

Most normal metal oxide for methane reforming, for example, α- and γ-Al_2O_3, MgO, $MgAl_2O_4$, SiO_2, ZrO_2, TiO_2, CeO_2, La_2O_3, and CaO have been utilized as support materials. These supports have great porosity, which permits bigger surface region. Support assumes an urgent part since it focus the last molecule size of the metal, with its pore structure, morphology, and stage moves that it can experience. Moreover, a support can have a chemical part too, by initiating one or more reaction steps (Liu, 2006).

Wang et al. demonstrated that solid interaction in the middle of metal and support would make a catalyst more impervious to sintering and coking, which would make a more steady catalyst (Wang & Lu, 1998).

Bradford et al. found that Ni-Ni bonds for Ni/MgO catalysts can be settled by NiO-MgO strong arrangement. Furthermore it can anticipate carbon dispersion into nickel particles. Likewise, they saw that the support impacts the catalyst action by changing the electron donating capacity of the lessened nickel surfaces. With the Ni/TiO_2 study, they found that an in number metal-support interaction happens, which would bring about blockage of the active nickel sites. These blockages are because of the relocation of TiO_x-species from the TiO_2-bearer (Bradford & Vannice, 1996).

These couple of illustrations demonstrate the impact of the support on catalysts. Nonetheless, a support can likewise partake in catalytic reaction. Supports with an essential nature, for example, MgO, are known not the activation of steam, and separation of steam into OH and H species. Carbon stores can prompt active site blocking and influence the catalyst reactivity and stability. The support can likewise assume a part in smothering carbon deposition. ZrO_2 and CeO_2 have been known able to oxidize stored carbon. Further, they are equipped for taking part in the catalytic reaction by oxidizing or diminishing reaction intermediates. Dong et al. considered methane reforming over $Ni/Ce_{0.15}Zr_{0.85}O_2$ catalysts. They concluded that there were two sorts of active sites that exist, one for methane activation and one for steam or oxygen activation. Ceria, can store, discharge, and exchange oxygen species, which brings about an upgraded capacity to avoid carbon formation (Dong, et al., 2002).

2.33 Nickel (Ni)

Among the catalysts examined, Ni is one of a good replacement for noble metals, due to its comparable catalytic performance and low cost in terms of methane conversion and selectivity to synthesis gas. However, Ni based catalysts are more easily deactivated, because of carbon deposition and active metal species sintering and carbon deposition cannot be avoided over nickel-supported catalysts and for a CO/CO_2 molar ratio of unity (Kroll, et al., 1996; Rostrup-Nielsen & Hansen, 1993).

From the past theory and experimental studies, it was affirmed that amount of Ni particles have a superior capacity to smother the carbon deposition (Xu, et al., 2011). By and by, binding the size of Ni particle inside of the nanoscale measurement is troublesome, on the grounds that the sintering of the Ni particles effectively happens under the serious reaction states of dry reforming of methane. As of late, it was accounted for that the tying down impact, an idea that was depicted by Yermakov, can encourage the arrangement of the active Ni nano-clusters with high dispertion under the reaction condition (Cai, et al., 2014).

For the most part, the catalyst utilized for the dry reforming of methane are arranged into two gatherings: (i) supported noble metals (Pt, Pd, Rh, Ru) and (ii) non-noble transition metals (Ni, Co, Fe). In examination to noble and other transition metals, Ni is by all accounts the most encouraging decision on the grounds that it is less expensive, and relatively more active and selective. However Ni based catalysts tend to deactivate because of sintering, coking, phase change and loss of active segment (Fan, et al., 2009).

Carbon decomposition has long been perceived as the principle explanation behind metal supported catalysts deactivation in methane reforming reaction. Various theory and experimental studies on dry reforming of methane instrument have uncovered that when dry reforming of methane procedure, methane is decayed first on active metal locales to frame responsive surface carbonaceous species close gas-metal interface, which are then oxidized to CO by collaborating with oxygen that started from CO_2 (Huirache-Acuña, et al., 2013). In perspective of that, the rate of coke deposition on catalyst surface is reliant on the relative rates of the carbon formation and its oxidative removal. Thus, if the rate of the carbon gasification by CO_2 is not exactly the rate of carbon formation, the huge volume of carbon deposit will amass over gas-metal interface, which can thereafter polymerize. These polymerized carbon particles can add to catalysts deactivation through two ways: (i) embodying the active metal particles or diffusing through the active metal subsequent to dissolving, and (ii) isolating active metal particles from the support (Cai, et al., 2014). It is accepted that the carbon formation is more effortlessly supported by acidic supports than essential support and also, coke deposition happens more effectively on greater particles than littler ones.

Since Ni molecule size and its dispersion over support has an in number impact on catalyst deactivation and carbon deposition. CO beat chemisorption analyses were done to watch the progressions in Ni molecule size and their circulation. The most noteworthy active metal

dispersion and littlest metallic crystallite size were achieved for Ni, which were in charge of its better strength and resistance towards coking. While among all the tried catalysts most reduced Ni dispersion and greatest Ni crystal size were seen in the event of Ni-Ce catalyst. Actually the most noteworthy coke deposition if there should arise an occurrence of Ni-Ce catalyst is because of the vicinity of greater Ni molecule in this catalyst (Cai, et al., 2014).

2.4 Santa Barbara Amorphous 15 (SBA-15)

Santa Barbara Amorphous 15 silica (SBA-15) shows fascinating textural properties, for example, huge particular surface areas (over 1000 $m^2 \cdot g^{-1}$), uniform-sized pores (in range 4–30 nm), thick system walls, little crystallite size of essential particles and reciprocal textural porosity. The upsides of SBA-15 material as support incorporates likewise its high surface-to-volume ratio, variable structure creations and high thermal stability (Huirache-Acuña, et al., 2013). Mesoporous silicas, for example, SBA-15 have an alternate pore structure from mesoporous aluminas. Mesoporous silicas show common sort IV isotherms and steep hysteresis circles (sort H1) at high relative weight, demonstrating a huge and tube shaped pore structure (Kima, et al., 2007).

Figures 5(a) and 5(b) shows two high determination transmission electron microscopy (HRTEM) micrographs of research center synthetized SBA-15 mesoporous silica calcined at 550°C. The SBA-15 shows hexagonal pores in a 2D exhibit with long 1D channels (p6mm plane gathering) (Zhang, et al., 2005). The channels are interconnected by little micropores. Subsequently, SBA-15 displays essentially mesoporous structure and has a little amount of micropores. The huge pore size of this mesoporous material can alleviate the dispersion boundary for the reactants and the items. On the other hand, pure siliceous SBA-15 has an electronically unbiased structure and needs Brønsted corrosiveness. This issue could be evaded by SBA-15 alteration with a specific end goal to make this mesoporous substrate more adaptable as far as its conceivable applications, either as a basic material or support, in adsorption processes, separation, catalysis or as evaluated for this situation, as support of catalysts utilized as a part of hydrodesulfurization (HDS) reactions in petroleum refining procedures (Huirache-Acuña, et al., 2013).

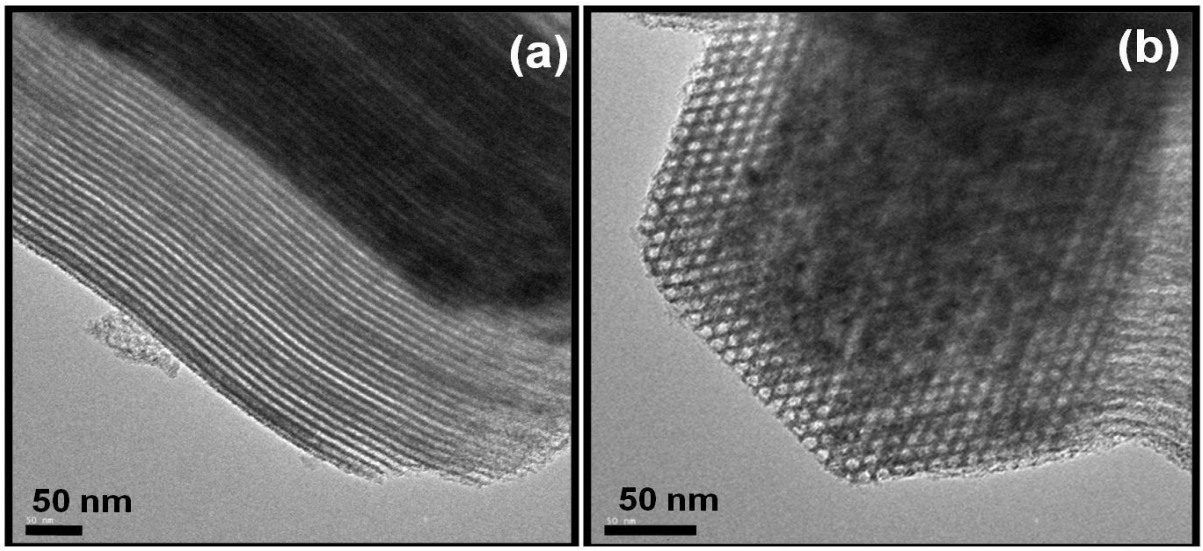

Figure 2.3: High resolution transmission electron microscopy (HRTEM) micrographs of SBA-15 mesoporous silica. The size and morphology of the highly ordered hexagonal pores in a 2D array (a) with long 1D channels (b) (p6mm plane group) can be observed.

There are numerous ways to deal with plan better SBA-15-supported catalysts, for example, replace the support properties by substitution of Si^{4+} by distinctive cations, functionalization with diverse groups, and so forth, changing the active stage part, differing the preparation system, and so on. By and large, the studies in this field plan to get connections between distinctive physical and substance properties of the support and active stages and catalyst execution for hydrotreating reactions, for example, hydrodesulfurization (HDS), hydrodenitrogenation (HDN), hydrodeoxygenation (HDO) and/or hydrodearomatization (HDA). Late correction by Rahmat et al. on the SBA-15-based catalysts centered with respect to the application in biorefinery generation (Rahmat, et al., 2010).

While trying to grow new more compelling mesoporous silica support, the (HDS) action of SBA-15-supported catalysts were contrasted and those supported on hexagonal mesoporous silica (HMS) and SBA-15 demonstrating diverse morphology and pore diameter. The SBA-15 has altogether bigger pore diameter than those of HMS and SBA-16, and both SBA-15 and SBA-16 substrates are steadier than HMS, because of their thicker pore dividers (Huirache-Acuña, et al., 2013). Interestingly, it was found that the catalytic reaction of HMS- and SBA-15-supported catalysts in the HDS reaction of DBT was comparative. This was a shocking result, in light of the fact that, in correlation with the HMS, the SBA-15 demonstrated a bigger pore diameter. The comparable HDS activity of both HMS- and SBA-15-based catalysts may demonstrate that the wormhole mesostructure of HMS offers comparative

transport for reactants and items than uniform tubular channels of SBA-15 (Nava, et al., 2009). Be that as it may, the study by Dimitrov et al. proposed that SBA-15 ought to be more successful as support than its HMS partner (Dimitrov, et al., 2011). The activity pattern reported by those creators for NiW catalysts, tried in the HDS of thiophene, is: NiW/W-SBA-15 > NiW/W-HMS > NiW/γ-Al2O3. Since the sort of active stages (CoMo versus NiW) and forerunners (heptamolybdate against heteropoly-acids) are distinctive in these two works and as it was exhibited that channels of the SBA-15 could be extended to oblige metal sulfide stages, it can't be said what support is better for supporting HDS catalysts (Kónya, et al., 2007; Vradman, et al., 2003).

Uses of amphiphilic triblock copolymers in 1998 was to direct the syncronization of polymerizing silica species was contemplated by B. F. Chmelka and G. D. Stucky et al. also, they was brought about the planning of all around requested hexagonal SBA-15 (Chmelka, et al., 1998). SBA-15 is a type of ordered mesoporous silica with large pore diameter, thick wall, good hydrothermal stability, and larger surface area. In 2006, dry reforming of methane using a Ni/SBA-15 catalyst was investigated by L.I. Chengyue et al. They reported that the 12.5% Ni/SBA-15 catalyst showed high activity and good stability at 800°C (Meili, et al., 2006; Chengyue, et al., 2007). In 2012, dry reforming catalyst was done by W. Yang and Z. Liu et al. that used a kind of Ni containing mesoporous silica, Ni/KIT-6 (Liu, et al., 2012).

In their work, a comparison study on methane dry reforming with carbon dioxide over Ni supported on mesoporous SBA-15, MCM-41, KIT-6 and sol-gel prepared g-Al_2O_3 has been investigated. This involved evaluation of methane and CO_2 conversions using a custom built catalysis rig. Activity and stability results were compared and are discussed based on the characterisation data obtained (Amin, et al., n.d.).

Nowadays, three types of siliceous materials with different structure have been investigated as support materials for Ni dry reforming catalysts. These materials, MCM-41, SBA-15 and KIT-6 are silica-based mesoporous materials with different pore diameter and surface area (Amin, et al., n.d.). In 1992, MCM-41 mesoporous molecular sieves had been synthesized by C. T. Kresge and coworkers by a liquid-crystal template mechanism. (Kresge, et al., 1992) These materials presented an opportunity for the design of catalytically active sites inside uniform channels with controllable nano-size pore diameters.

2.5 Ni supported by SBA-15 (Ni/SBA-15)

Numerous efforts have been devoted toward improving the catalytic properties of nickel-based catalysts. Ni/Al_2O_3 catalysts promoted with MgO and CeO_2 appeared to be more resistant to carbon deposition in dry reforming of methane due to the high Ni dispersion and low dehydrogenation activity (Xu, et al., 1999). The catalytic behavior of Ni/Ce-SBA-15 had been improved to the incorporation of cerium into the framework of SBA-15, which promoted the dispersion of nano-sized Ni species and inhibited the carbon formation (Wang, et al., 2012). The mesoporous $Ni-Al_2O_3$ catalyst prepared by the one-pot method presented better long-term stability than that of the Ni-impregnated one as reported by Wang *et al*. The enhancement of the catalytic stability was closely associated with the stabilization of the active nickel particles by alumina support (Wang, et al., 2013). Liu *et al*. was founded that the high conversion and catalytic stability over Pt-impregnated Ni/MCM-41 catalyst were due to the strong interaction between Pt and nickel species within the SiO_2 matrix (Liu, et al., 2010).

From the past experiment, the catalytic properties of nickel has mesoporous molecular sieve catalysts for dry reforming of methane. Ni/MCM-41 catalysts exhibited steady and better improving activity rather than the impregnated catalyst. Moreover, a somewhat higher activity was seen under He pretreatment as opposed to H_2 enactment amid security test. The enhanced catalytic execution of Ni/MCM-41 under He pretreatment was firmly identified with the littler active sites metal destinations being balanced out by the silica grid and/or the encompassing unreduced nickel particles. In this manner, there is a low propensity toward carbon deposition (Liu, et al., 2009).

Through the presentation of Zr into Ni/MCM-41, an improved starting activity and a long haul security were discovered while such impact was not present over Ti^- and manganese–nickel doped Ni-based catalysts. It was confirm that Zr^{4+} improved the structure stability and the dispersion of active Ni sites. The solid tying down impact of Zr^{4+} and fractional actuation of CO_2 by Zr^{4+} added to the prevalent catalytic properties. It is all around perceived that the pretreatment conditions are fundamental for the formation of active metal destinations subsequently influencing their catalytic exhibitions (Liu, et al., 2009).

Prior reports have demonstrated the diminishment of nickel oxide to nickel is practical by CO (Budarin, et al., 1998) and CH_4 (Alizadeh, et al., 2007) in spite of the development of some carbon amid this procedure. In the perspective of the reasonable application, contrasted with H_2, the three gasses CO, CH_4 and He are of more huge practical point of interest. In the present commitment, ZrO_2/SiO_2 supported Ni catalyst was arranged by deposition-precipitation technique. The impact of pretreatment under different gasses, for example, He, CO, CH_4 and H_2 on the dry reforming of methane was examined. Some understanding into the deactivation components amid dry reforming was acquired through a few portrayal systems (Liu, et al., 2012).

From the results presented in Figures 6(a) and 6(b) below (Amin, et al., n.d.), the Ni/SBA-15 catalyst was clearly more active in terms of methane and CO_2 conversion than all of the other materials tested. This catalyst was able to catalyse CH_4 conversions is 84.8% and a CO_2 conversion of 92.4 % throughout for the 2 h experiment. The CH_4 conversion approached the conversion expected for the system at thermodynamic equilibrium which is 91.5% (the reaction condition used were CH_4/CO_2=1 at 700 ^oC and atmospheric pressure) (N. Wang, 2012). The CO_2 conversion was higher than that expected if the system was at thermodynamic equilibrium (66.3%) (Khoshtinat & Amin, 2011), due to the influence of the reverse water gas shift (RWGS) reaction, which has been reported to occur under the experimental conditions used in this study (Newnham, et al., 2012).

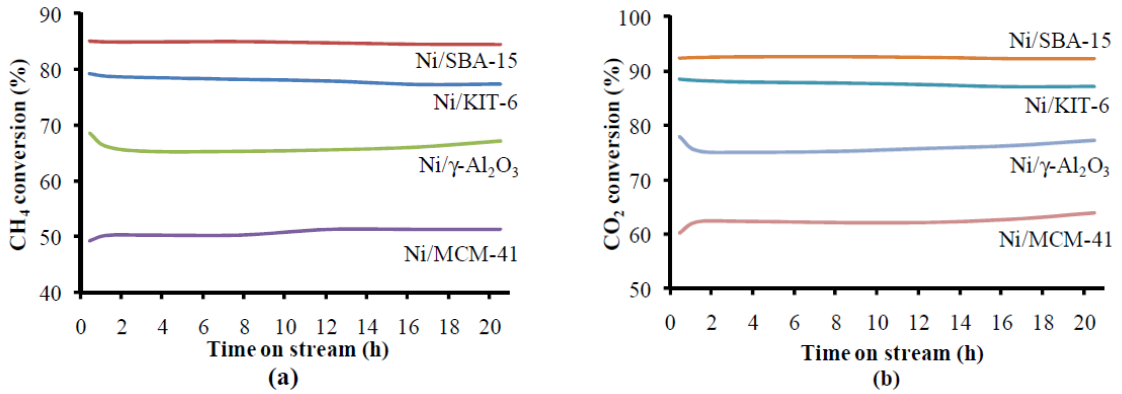

Figure 2.4: The effect of support on CH_4 (a) and CO_2 (b) conversion over Ni catalysts at 700°C and at GHSV of 52,000 mL $h^{-1}g^{-1}$.

Thus, we choose SBA-15 as catalyst support by Ni to be loaded due to large pore diameter, thick wall, good hydrothermal stability, and larger surface area. This catalyst expected to enhance the CO_2 and CH_4 conversion with high yield of syngas.

3.0 MATERIALS AND METHODS

3.1 Overview

This chapter describes overview on the procedure involved in this research. The SBA-15 will be synthesized by conventional method. Whereas, Ni/SBA-15 will synthesized via impregnation method. The characterization of catalyst and catalytic activity testing for the catalyst also described in this chapter.

3.2 Methodology

3.21 Materials

The chemicals using are Poly(Ethylene Glycol)-block-Poly(Propylene Glycol)-block-Poly(Ethylene Glycol), Pluronic P-123, Tetraethyl Orthosilicate (TEOS), Hydrochloric acid (HCL 37% purity) and Nickel Nitrate Hexahydrate ($Ni(NO_3)_2$). This chemical were obtained from Merck Malaysia.

3.22 Synthesis of catalyst

3.221 Synthesis of SBA-15 by conventional method

In a preparation experiment 9.8g of triblock copolymer Poly(Ethylene Glycol)-block-Poly(Propylene Glycol)-block-Poly(Ethylene Glycol) / P123 (average molecular weight = 5800) was dissolved in 313 mL of deionized water and 40 mL oh Hydrochloric Acid (HCL, 37 wt%) and stirred for 1 h at 40^{o}C. P123 was completely dissolved when clear solution formed. And then, 21.7g of Tetraethyl Orthosilicate (TEOS) was added to the clear solution and aged with stirring at 40^{o}C for another 24 h. the obtained precipitate was filtered, washed and dried overnight at 110^{o}C. The dried white powder was calcined in air at 550^{o}C for 6h to remove the triblock copolymer. The SBA-15 used in this study was successfully synthesized via a simple conventional method.

3.222 Synthesis of Ni/SBA-15 by impregnation method

Ni/SBA-15 catalysts, with 1 wt%, 3 wt% to 5 wt% nickel content, were prepared by the impregnation method. To prepare the Ni-SBA-15 catalyst, calculated amount of Nickel Nitrate Hexahydrate need to be dissolved in 53 mL deionized water. Next, 9.7g SBA-15 need to be added to the above solution for 12 h. The mixture need to be dried at 105°C in air for 12 h. The above resultant solids after drying need to be calcined in air for 5 h at 550 ^{o}C before catalytic activity tests (Jun, et al., 2013).

3.23 Characterization of catalysts

- X-ray diffraction (XRD) will be used to characterize the material structure, crystalline lattice and composition.
- Thermogravimetric Analysis (TGA) will be used to measure weight changes in a material as a function of temperature (or time) under a controlled atmosphere. Its principle uses include measurement of a material's thermal stability, filler content in polymers, moisture and solvent content, and the percent composition of components in a compound.
- Transmission Electron Microscope (TEM) will be used to collect the structure images of catalysts.
- Brunauer–Emmett–Teller, Autosorb-1, Quantachrome (BET) will be used to analyze the surface area and pore size of catalysts by nitrogen adsorption and desorption isotherms. The sample was degassed at 100^{o}C to remove the adsorbed water and impurities before measurement.

3.24 Catalytic activity testing

CO_2 reforming of methane was conducted in a glass tube reactor fitted in a square furnace. In a typical CO_2 reforming of methane reaction, 0.15 g of catalyst with 1wt%, 3wt% and 5wt% Ni content was loaded into the glass reactor. The catalyst was heated until 700^{o}C and introduce the methane, CO_2 and H_2 gas at 700^{o}C until 3 hours experiment. The effluent mixed gases were cooled in an ice-water trap to remove gaseous water generated via the reverse water gas shift (RWGS) reaction. Product collected using sample bag and directly analysed by gas chromatography. Methane conversion (X_{CH4}), CO_2 conversion (X_{CO2}) and the H_2 production yield (Y_{H2}) were calculated for each Ni content using the gas composition measured by GC:

$$X_{CH_4} = \left(\frac{F_{CH_4in} - F_{CH_4out}}{F_{CH_4in}}\right) \text{x } 100$$

$$X_{CO_2} = \left(\frac{F_{CO_2in} - F_{CO_2out}}{F_{CO_2in}}\right) \text{x } 100$$

$$Y_{H_2} = \left(\frac{F_{H_2out}}{2 \text{ x } F_{CH_4in}}\right) \text{x } 100$$

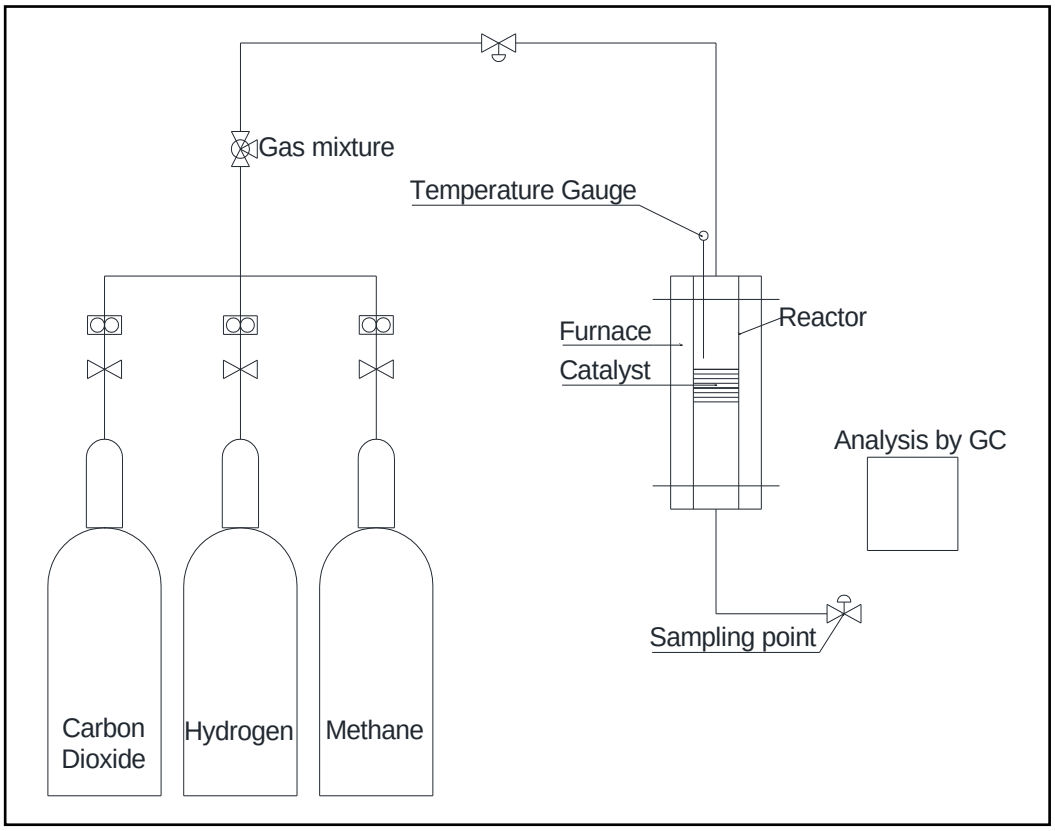

Figure 3.1: Schematic diagram of the reactor set-up.

4.0 RESULT AND DISCUSSION

4.1 Overview

This chapter will presented about CO_2 reforming of methane with present of hydrogen by reacting CO_2 and methane over Ni/SBA-15 catalysts. Ni/SBA-15 catalysts have been prepared using SBA-15 supports with different Ni weight percent (wt%) synthesized by impregnation method. CO_2 reforming of methane was conducted in a glass tube reactor fitted in a square furnace for the catalyst activities. And also, Ni/SBA-15 with 1wt%, 3wt% and 5wt% Ni content catalysts have been characterized by X-ray diffraction (XRD), Brunauer–Emmett–Teller, Autosorb-1, Quantachrome (BET), and Thermogravimetric Analysis (TGA).

4.2 Catalytic activity testing

Figures 8 and 9 compared the catalytic performances of CO_2 and CH_4 conversion for the 1wt%, 3wt% and 5wt% Ni content in Ni/SBA-15 for the CO_2 reforming of methane in the time-on-stream at 700°C. In both figure, CO_2 and CH_4 conversions show that 3 wt% of Ni content is the best result because of time taken to achieve stable. Based on both graph, 3 wt% of Ni content shows 0.5 h early then 5 wt% of Ni content to stable. In addition, 3 wt% of Ni content is more preferable because of less Ni content used as a catalyst for CO_2 reforming of methane.

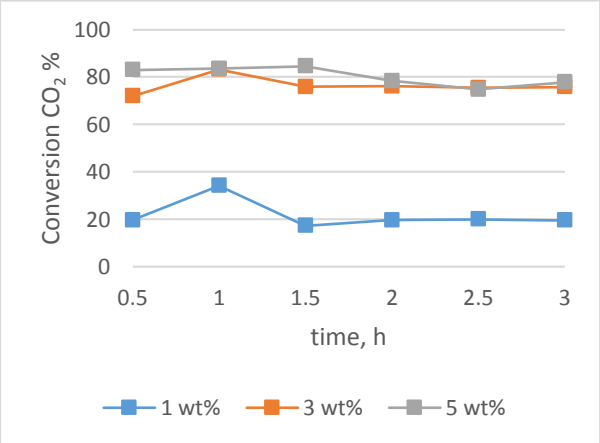

Figure 4.1: Graph of CO_2 conversion at 700°C for 1, 3, and 5 wt% Ni content.

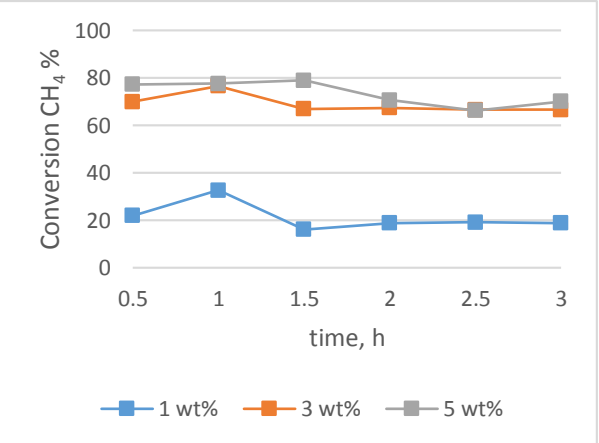

Figure 4.2: Graph of CH_4 conversion at 700°C for 1, 3, and 5 wt% Ni content.

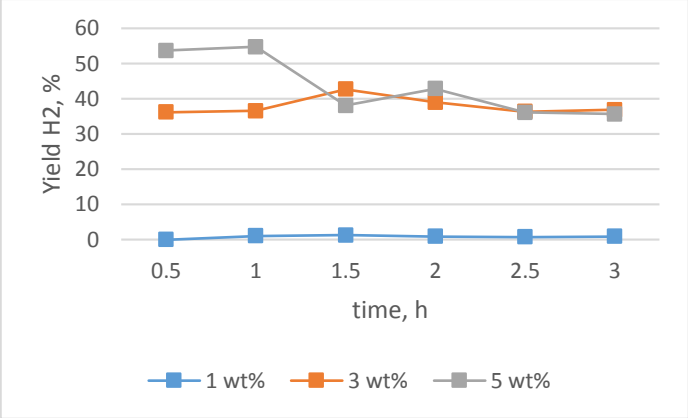

Figure 4.3: Graph yield of H_2 at 700°C for 1, 3, and 5 wt% Ni content.

Figure 10 shows the hydrogen production rate for CO_2 reforming of methane with 1wt%, 3wt% and 5wt% Ni content in Ni/SBA-15 catalysts. An increase of Ni content, it show that same hydrogen production rate over these catalysts exhibit remarkable catalytic activities. Higher the catalytic activity of Ni/SBA-15 catalysts was related to the high dispersion of Ni particles and the large BET surface area. Based on the discussion above, Rostrup-Nielsen et al. was conclude that the activity of the catalyst per unit metal surface area decreases with increasing of dispersion (i.e., with smaller metal crystal size) (Rostrup-Nielsen, 1989). Among these Ni content, 3 wt% of Ni content in Ni/SBA-15 is observed to give the highest H_2 production rate than 5 wt%. This is because 3 wt% is more stable in increase of time for long period.

4.3 Thermogravimetric analysis (TGA) testing

TGA was used to determine the weight loss of the sample material when it was heated at constant heating rate of 10°C/min from room temperature to 800°C.

Figure 11 shows the TGA curves characterizing the weight loss, (%) of Ni/SBA-15 when 1wt%, 3wt% and 5wt% Ni loading on SBA-15 after 3 hour of CO_2-methane reforming reaction. The TGA curve initially experienced a slight decrease in the region below 100°C. For the second weight loss decrease a little bit at 230°C – 410°C related to desorption of chemical bonded of water molecule. At temperature 700°C, Ni loading on SBA-15 has a slight enhancement in thermal stability of catalyst and also was a good for the reaction occur for the catalyst.

It could be clearly observed that the weight loss of the carbon deposition over the used 3 wt% of Ni content in Ni/SBA-15 was much higher than that over the used 5 wt% of Ni content in Ni/SBA-15. For dry reforming processes, carbon deposits mostly to be produced and block active sites or/and the catalyst pores that are responsible for a high active surface. Hence, the weight losses from 49°C to 900°C are caused probably derived from the oxidation of Ni particles.

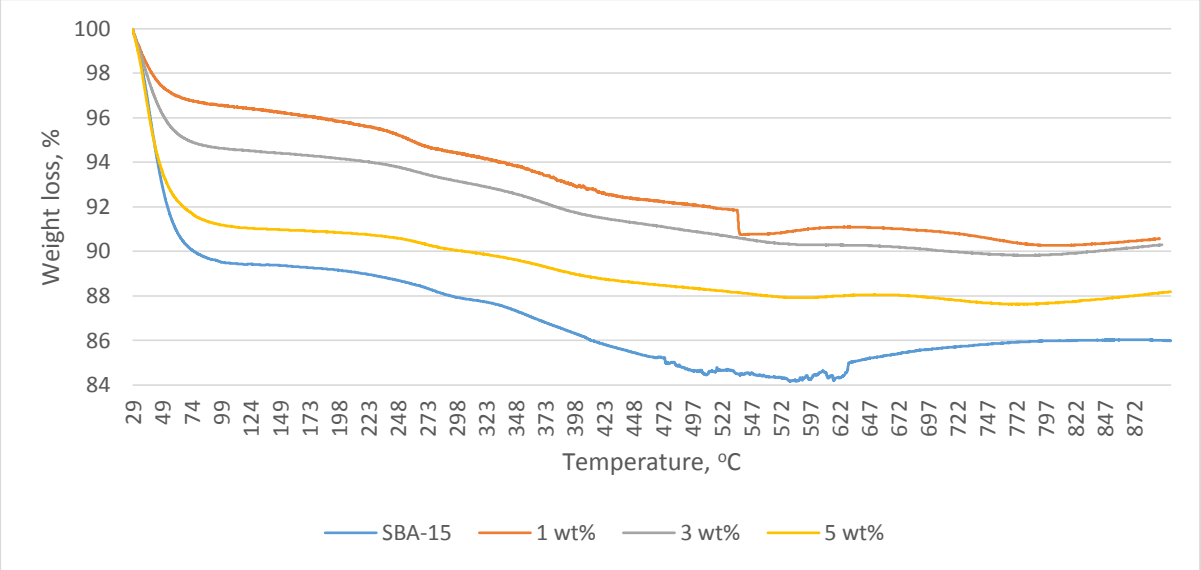

Figure 4.4: TGA graph of 1wt%, 3wt% and 5wt% Ni content.

4.4 X-Ray diffraction (XRD) testing

XRD (X-ray diffraction) was used to characterize the material structure, crystalline lattice and composition. The XRD patterns was used a continuous scan angle 2θ was selected from 3º to 80º. A divergence slit was inserted between the X-ray and the sample to ensure the interaction of X-ray beam with the sample.

The small angle XRD patterns of Ni/SBA-15 catalysts did not show the existence of nickel particles in Figure 12 because of bigger catalyst size and less dispersion of Nickel. No obvious diffraction peak of nickel oxide can be identified for 1 wt%, 3 wt% and 5 wt% of Ni content in Ni/SBA-15, implying that most of the nickel species are in the silica framework or highly dispersed on the silica surface. This is in agreement with the observation over Ni-MCM-41 reported in the literature (Liu, et al., 2009).The characteristic XRD peaks of mesoporous structure with the 2θ values around 18°-30° can be observed over all SBA-15. The presence of

Nickel Oxide shows very small peak at 37.2°, 43.3° and 62.4° since the other peaks was overlapped with SBA-15 (Ibrahim, et al., 2014)

In general, the dispersion of active metal oxide, particle sizes, and interaction between active metal and supports can affect the reducibility of active metal (Xusheng & Kawi, 2009). It may be for that reason NiO species are not distinguishable due to the high level of dispersion on the support. This came in accordance with results of the catalytic test, from which it was observed that when the Ni content was increased, the catalytic performance remain same. This brought us to conclude that a small amount of the promoter is preferred (Habimana, et al., 2009).

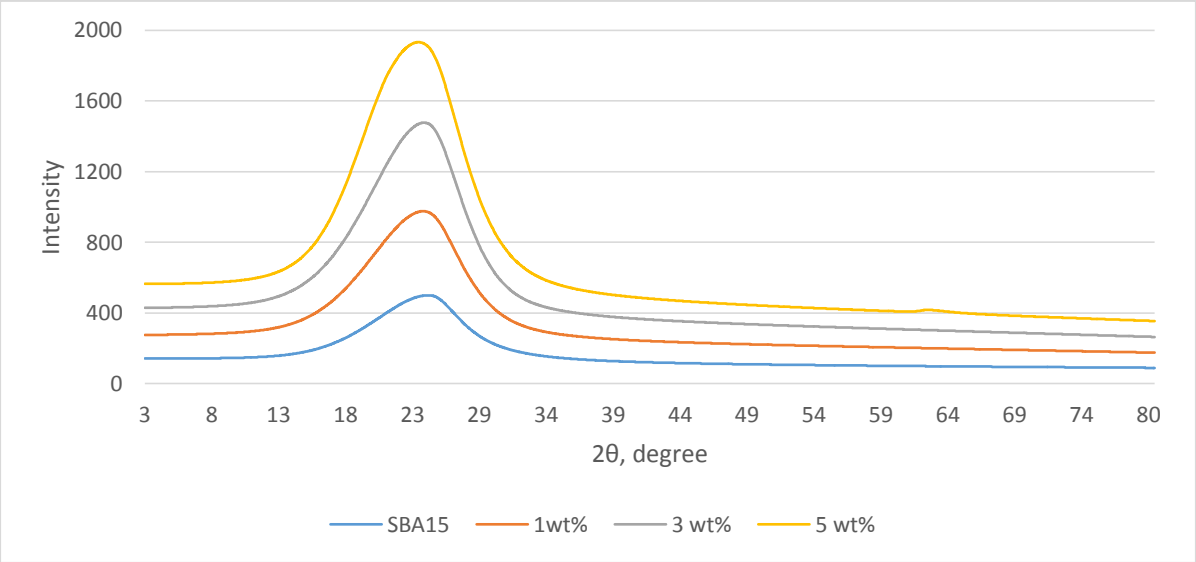

Figure 4.5: XRD pattern of 1wt%, 3wt% and 5wt% Ni content.

4.5 Brunauer–Emmett–Teller, Autosorb-1, Quantachrome (BET) testing

BET (Brunauer–Emmett–Teller, Autosorb-1, Quantachrome) was used to analyze the surface area and pore size of Ni/SBA-15 (1, 3, 5 wt%) catalysts by nitrogen adsorption and desorption isotherms. The sample was degassed at 100°C to remove the adsorbed water and impurities before measurement.

The N_2 adsorption-desorption isotherms of the 1 wt%, 3 wt% and 5 wt% of Ni content in Ni/SBA-15 are shown in Table 1. All isotherms exhibit typical IV-type isotherms with a sharp increase of nitrogen uptake in the relative pressure range of 0.6–0.82, which is caused by

capillary condensation of nitrogen inside uniform mesopores. The decreased surface area and pore volume coincide with the increase of nickel loading. However, the surface area of 3 wt% of Ni content Ni/SBA-15 show the higher surface area between 1 wt% and 5 wt% of Ni content.

As shown in Table 1, the pore diameters of 3 wt% of Ni content Ni/SBA-15 increase gradually with the increase of Ni content, showing the incorporation of Ni into the framework of SBA-15. The pore diameter then starts to decrease when 5 wt% of Ni content Ni/SBA-15 due to the formation of nickel oxide nanocrystallites outside the mesopores (Xusheng & Kawi, 2009).

However, the pore diameter and specific surface area drop significantly from 3 wt% to 5 wt% of Ni content Ni/SBA-15. The N_2 adsorption results are in good agreement with the XRD results, which show the incorporation of Ni content into the mesoporous framework of SBA-15. Similar studies have been reported over several mesoporous silica supports incorporated with Mg (Xusheng & Kawi, 2009).

Table 4.1: Structural and textural properties of SBA-15 and Ni-SBA-15 with different wt% of Ni content.

Catalyst	Surface area (m^2/g)	Pore diameter (nm)	Pore volume (cm^3/g)
Pure SBA-15	1631.4	7.12	1.50
1 wt%.Ni/SBA-15	311.6	6.83	1.06
3 wt%.Ni/SBA-15	1833.7	6.50	1.24
5 wt%.Ni/SBA-15	1024.7	6.80	0.76

5.0 CONCLUSION AND RECOMMENDATION

5.1 Conclusion

Ni/SBA-15 catalyst was successfully synthesized for catalytic performance CO_2 reforming of methane. The effects of SBA-15 support, Ni as an active metal, Ni/SBA-15 in different loading arrangement were important factors that influenced the characteristics and the performance of catalyst.

Based on the results obtained, the effects of conversion and yield in CO_2 reforming of methane were studied for fundamental understanding due to suitable properties that applied in this research. From the supported catalysts tested, Ni/SBA-15 exhibited excellent catalytic performance in terms of conversion and yield. Based on the results, 3 wt% of Ni content Ni/SBA-15 shows a good performance, surface area, pore diameter, stability, and good dispersion as a catalyst for dry reforming of methane. Also, impregnation method will be using to synthesis the catalyst and the result will be compared with another method.

5.2 Recommendation

The research carried in experiment is currently being expanded by Dr. Nurul Aini Binti Mohamed Razali. Focus for this new work will be on catalyst that used have more effective and good performance that has supported to produce H_2.

The following recommendations are suggested towards the improvement of the developed catalyst in the reforming carbon dioxide (CO_2) of methane to syngas reaction and its future studies.

1. The performance of the catalyst should be improve by using bimetallic metals to show the reaction be more effective, give optimum conversion of CO_2 and CH_4 with high yield of H_2.
2. The Ni loading can be higher than 20% should be considered in the future studies as the synthesized Ni/SBA-15 catalyst.

REFERENCES

Alizadeh, R., Jamshidi, E. & Ale-Ebrahim, H., 2007. Kinetics Study of Nickel Oxide Reduction by Methane. *Chemical Engineering Technology.*

Amin, M. H. et al., 2012. Highly Stable ytterbium Promoted Ni/γ-Al2O3 Catalysts for Carbon Dioxide Reforming of Methane. *Applied Catalyst ,* Volume 119– 120, p. 217–226.

Amin, M., James, T. & Bhargava, S., n.d. *A Comparison Study on Carbon Dioxide Reforming of Methane Over Ni Catalysts Supported on Mesoporous SBA-15, MCM-41, KIT-6 and g-Al2O3,* Melbourne, Australia: RMIT University.

Barker, S. & Elderfield, H., 2002. Foraminiferal Calcification Response to Glacial-Interglacial Changes in Atmospheric CO2. *Science 2,* Volume 297, pp. 833-836.

Bhd., S. S., n.d. *Syngas Renewable Energy.* [Online]
Available at: http://www.syngas.com.my/index.html
[Accessed 24 August 2014].

Böhringer, C., 2002. *The Kyoto Protocol: A Review and Perspectives.* [Online]
Available at: ftp://ftp.zew.de/pub/zew-docs/dp/dp0361.pdf
[Accessed 2014].

Bradford, M. & Vannice, M., 1996. Catalytic reforming of methane with carbon dioxide over nickel catalysts I. Catalyst characterization and activity. *Applied Catalysis A: General,* 142(1), pp. 73-96.

Bradford, M. & Vannice, M., 1999. Carbon Dioxide reforming of methane. Volume 41, p. 1–42.

Breen, J. P., Burch, R. & Coleman, H., 2002. Metal-Catalysed Steam Reforming of Ethanol in the Production of Hydrogen for Fuel Cell Applications. *Applied Catalyst B: Environmental,* Volume 39, pp. 65-74.

Brinckerhoff, P., 2011. *Accelerating the uptake of CCS: industrial use of captured carbon dioxide.* New York: Global CCS Institute.

Buchner, B., Carraro, C. & Cersosimo, I., 2002. Economic consequences of the US withdrawal from the Kyoto/Bonn Protocol. *Climate Policy*, 2(4), pp. 273-292.

Budarin, V. et al., 1998. Peculiarities of the reduction of NiO with carbon monoxide associated with a magnetic phase transition in nickel.

Butterfield, A. B., 2013. *New Energy News - World Still Building the Hydrogen Hiway.* [Online]
Available at: http://newenergynews.blogspot.com/2013/11/world-still-building-hydrogen-hiway.html
[Accessed 3 12 2014].

Cai, W. et al., 2014. Highly Dispersed Nickel-Containing Mesoporous Silica with Superior Stability in Carbon Dioxide Reforming of Methane: The Effect of Anchoring. *Materials,* Volume 7, pp. 2340-2355.

Chauvel, A. & Lefebvre, G., 1989. *Petrochemical Processes, 1 Synthesis-Gas Derivatives and Major Hydrocarbons.* Paris: Éditions Technip.

Chengyue, L., Shengfu, J., Pingyi, W. & Linhua, H., 2007. Preparation and Catalytic Applications of Transition Metal Assembled into the Channels of Mesoporous Molecular Sieves. *Progress in Chemistry,* Volume 19, pp. 437-443.

Chen, Y. G., Tomishige, K., Yokoyama, K. & Fujimoto, K., 1999. Catalytic Performance and Catalyst Structure of Nickel–Magnesia Catalysts for CO2 Reforming of Methane. *Journal Catalyst,* Volume 184, pp. 479-490.

Chmelka, B. F. et al., 1998. Continuous Mesoporous Silica Films with Highly Ordered Large Pore Structures. *Advanced Materials,* 10(16), pp. 1380-1385.

Christensen, T. & Primdahl, I., 1994. Improve synthesis gas production using auto thermal reforming. *Hydrocarbon Processing,* pp. 39-46.

Chubb, T. A., 1980. Characteristics of CO2-CH4 reforming-methanation cycle relevant to the solchem thermochemical power system. *Solar Energy,* Volume 24, pp. 341-345.

Dimitrov, L., Palcheva, R., Spojakina, A. & Jiratova, K., 2011. Synthesis and characterization of W-SBA-15 and W-HMS as supports for HDS. *Journal of Porous Material,* Volume 18, pp. 425-434.

Dong, W.-S.et al., 2002. Methane reforming over Ni/Ce-ZrO2 catalysts: effect of nickel content. *Applied Catalysis A: General,* 226(1-2), pp. 63-72.

Enzler, S., 2014. *History of the greenhouse effect and global warming.* [Online] Available at: http://www.lenntech.com/greenhouse-effect/global-warming-history.htm#ixzz3F11MrO4i
[Accessed 3 October 2014].

Fan, M., Abdullah, A. & Bhatia, S., 2009. Catalytic technology for carbon dioxide reforming of methane to synthesis gas. *Chemical Catalyst,* Volume 1, p. 192–208.

Feely, R., Wanninkhof, R., Takahashi, T. & Tans, P., 1999. Influence of El Niño on the equatorial Pacific contribution of atmospheric CO2 accumulation. *Nature,* Volume 398, pp. 597-601.

Ferreira-Aparicio, P., Guerrero-Ruiz, A. & Rodroguez-Ramos, I., 1998. Comparative study at low and medium reaction temperatures of syngas. *Applied Catalyst,* Volume 170, pp. 177-187.

Fierro, V., Klouz, V., Akdim, O. & Mirodatos, C., 2002. Oxidative Reforming of Biomass Derived Ethanol for Hydrogen Production in Fuel Cell Applications. *Catalyst Today,* Volume 75, pp. 141-144.

Fischer, V. & Tropsch, H., 1928. *Brennstoff-Chemie.* 3 ed. s.l.:s.n.

Habimana, F. et al., 2009. Effect of Cu promoter on Ni-based SBA-15 catalysts for partial oxidation of methane to syngas. *Journal of Natural Gas Chemistry,* Volume 18.

Huirache-Acuña, R. et al., 2013. SBA-15 Mesoporous Silica as Catalytic Support for Hydrodesulfurization Catalysts—Review. *Materials,* Volume 6, pp. 4139-4167.

Ibrahim, D., Adnan, M. & Haydar, K., 2014. *Progress in Sustainable Energy Technologies: Generating Renewable Energy.* s.l.:Springer.

Jin-Kwon, L. et al., 2007. Catalytic Behavior of Nickel Particles Embedded in Three-dimensional Mesoporous SBA15. *Bull. Korean Chem. Soc.,* 28(1).

Jin-Kwon, L. et al., 2007. Catalytic Behavior of Nickel Particles Embedded in Three-dimensional Mesoporous SBA15. *Bull. Korean Chemical,* 28(1), p. 121.

Jun, T. et al., 2013. Catalytic Steam Reforming of Toluene as a Model Compound of Biomass Gasification Tar Using Ni-CeO2/SBA-15 Catalysts.

Khoshtinat, M. & Amin, N., 2011. Thermodynamic analysis of carbon dioxide reforming of methane in view of solid carbon formation. *Fuel Process Technology,* Volume 92, p. 678–691.

Kima, P. et al., 2007. Preparation of nickel-mesoporous materials and their application to the hydrodechlorination of chlorinated organic compounds. *Catalysis Surveys from Asia,* Volume 11, pp. 49-58.

Knutson, T., Tuleya, R. & Kurihara, Y., 1998. Simulated increase of hurricane intensities in a CO2-warmed climate. *Science,* Volume 1018-1020, p. 279.

Kónya, Z. et al., 2007. Pre-prepared platinum nanoparticles supported on SBA-15—Preparation, pretreatment conditions and catalytic properties. *Catalyst Letter,* Volume 113, p. 19–28.

Korada, S., Sumaeth, C., Lance, L. L. & Richard, G. M., 2002. CARBON DIOXIDE REFORMING WITH METHANE IN LOW TEMPERATURE PLASMAS. *Fuel Chemistry Division Preprints,* Volume 47(1), pp. 269-270.

Kresge, C. T. et al., 1992. Ordered mesoporous molecular sieves synthesized by a liquid-crystal template mechanism. *Nature,* Volume 359, pp. 710-712.

Kroll, V., Swaan, H. & Mirodatos, C., 1996. Methane reforming reaction with carbon dioxide over Ni/SiO2 catalyst 1. *Deactivation studies. J. Catalyst,* Volume 161, p. 409–422.

Lee, D. W., Yu, C. Y. & Lee, K. H., 2008. Study on Hydrothermal Stability and Catalytic Activity of Nanosphere-Walled Mesoporous Silica. *Journal of Physical Chemistry C,* Volume 112, pp. 5136-5140.

Lin, S., Harada, M., Suzuki, Y. & Hatano, H., 2002. Hydrogen Production from Coal by Separating Carbon Dioxide during Gasification. *Fuel,* Volume 81, p. 2079–2085.

Liu, D. et al., 2010. A comparative study on catalyst deactivation of nickel and cobalt incorporated MCM-41 catalysts modified by platinum in methane reforming with carbon dioxide. *Catalyst Today,* Volume 154, p. 229–236.

Liu, D., Lau, R., Borgna, A. & Yang, Y., 2009. Carbon dioxide reforming of methane to synthesis gas over Ni-MCM-41 catalysts. *Applied Catalyst.*

Liu, D. et al., 2009. MCM-41 supported nickel-based bimetallic catalysts with superior stability during carbon dioxide reforming of methane: effect of strong metal-support interaction. *Journal Catalyst,* Volume 266, pp. 380-390.

Liu, D. et al., 2012. Methane reforming with carbon dioxide over a Ni/ZiO2-SiO2 catalyst: Influence of pretreatment gas atmospheres. *Hydrogen,* Volume 37, pp. 10135-10144.

Liu, H. et al., 2008. Preparation, Characterization and Activities of the Nano-sized Ni/SBA-15 Catalyst for Producing COx-free Hydrogen from Ammonia. *Applied Catalyst,* Volume 337, pp. 138-147.

Liu, J. A., 2006. *Kinetics, Catalysis and Mechanism of Methane Steam Reforming,* s.l.: s.n.

Liu, Z. et al., 2012. Highly dispersed nickel loaded on mesoporous silica: One-spot synthesis strategy and high performance as catalysts for methane reforming with carbon dioxide. *Applied Catalyst,* Volume 125, p. 324– 330.

Maslin, M., 2004. *Global Warming, a very short introduction,* Oxford: Oxford University Press.

McKibbin, W. & Wilcoxen, P., 2002. The Role of Economics in Climate Change Policy. *Journal of Economic Perspectives,* 16(2), pp. 107-129.

Meili, Z. et al., 2006. Structural Characterization of Highly Stable Ni/SBA-15 Catalyst and Its Catalytic Performance for Methane Reforming with CO2. Volume 27(9), p. 777–782.

Montanez, I. et al., 2007. CO2-forced climate and vegetation instability during Late Paleozoic deglaciation.. *Science,* Volume 315, pp. 87-89.

Narasi, S. & Davion, H., 2011. *Carbon Dioxide Utilization: Electrochemical Conversion of CO2 – Opportunities and Challenges,* Høvik: s.n.

Nava, R. et al., 2009. Comparison of the morphology and reactivity in HDS of CoMo/HMS, CoMo/P/HMS and CoMo/SBA-15 catalysts. *Microporous Mesoporous Mater,* Volume 118, p. 189–201.

Newnham, J. et al., 2012. Highly stable and active Ni-mesoporous alumina catalysts for dry reforming of methane. *Hydrogen,* Volume 37(2), pp. 1454-1464.

Olah, G., Goeppert, A. & Prakash, G., 2009. Beyond Oil and Gas: The Methanol Economy.

On, D. T., Desplantier-Giscard, D., Danumah, C. & Kaliaguine, S., 2001. Perspectives in Catalytic Applications of Mesostructured Materials. *Applied Catalyst,* Volume 222, pp. 299-357.

Rahmat, N., Zuhairi, A. & Mohamed, A., 2010. A review: Mesoporous santa barbara amorphous-15, types, synthesis and its applications towards biorefinery production. *Applied Science,* Volume 7, p. 1579–1586.

Richardson, J., 1989. Principles of catalyst development. *Plenum Press,* pp. 28-31.

Riebesell, U. et al., 2000. Reduced calcification of marine plankton in response to increased atmospheric CO2.. *Nature,* Volume 407, pp. 364-367.

Rostrup-Nielsen, J. & Hansen, J., 1993. CO2 reforming of methane over transition metals. *Catalyst Today,* Volume 144, p. 38–49.

Rostrup-Nielsen, J. R., 1989. Catalytic Steam Reforming. *Catalysis: Science and Technology.*

Shah, P. & Ramaswamy, V., 2008. Thermal Stability of Mesoporous SBA-15 and Sn-SBA-15 Molecular Sieves: An in situ HTXRD Study. *Microporous and Mesoporous Materials,* Volume 114, pp. 270-280.

Shailesh, V., Jared, C. & Sean, P., 2013. Carbon Capture - Technology Program Plan. *Clean Coal Research Program.*

Sodesawa, T., Dobashi, A. & Nozaki, F., 1979. Catalytic reaction of methane with carbon dioxide. *Reaction Kinetics,* Volume 12(1), pp. 107-l 11.

Vizcaino, A. J., Carrero, A. & Calles, J. A., 2009. Ethanol Steam Reforming on Mg- and Ca-Modified Cu–Ni/SBA-15 Catalysts. *Catalyst Today,* Volume 146, pp. 63-70.

Vradman, L. et al., 2003. High loading of short WS2 slabs inside SBA-15: Promotion with nickel and performance in hydrodesulfurization and hydrogenation. *Catalyst Today,* Volume 213, p. 163–175.

Wang, N., Chu, W., Zhang, T. & Zhao, X., 2012. Synthesis, characterization and catalytic performances of Ce-SBA-15 supported nickel catalysts for methane dry reforming to hydrogen and syngas. *Hydrogen Energy,* Volume 37, p. 19–30.

Wang, N. et al., 2013. Facile route for synthesizing ordered mesoporous Ni-Ce-Al oxide materials and their catalytic performance for methane dry reforming to hydrogen and syngas. *ACS Catalyst,* Volume 3, p. 1638–1651.

Wang, S. & Lu, G., 1998. CO2 reforming of methane on Ni catalysts: Effects of the support phase and preparation technique. *Applied Catalysis B: Environmental,* 16(3), pp. 269-277.

Xu, G. et al., 1999. Studies of reforming natural gas with carbon dioxide to produce synthesis gas X. The role of CeO2 and MgO promoters. Volume 147, p. 47–54.

Xu, L., Song, H. & Chou, L., 2011. Carbon dioxide reforming of methane over ordered mesoporous NiO-MgO-Al2O3 composite oxides. *Applied Catalyst,* Volume 108, p. 177–190.

Xusheng, W. & Kawi, S., 2009. Rh/Ce-SBA-15:Active ans stable catalyst for carbon dioxide reforming of ethanol to hydrogen. *Catalyst Today,* Volume 148, pp. 251-259.

Zhang, F. et al., 2005. Understanding effect of wall structure on the hydrothermal stability of mesostructurated silica SBA-15. *Physical Chemistry,* Volume 109, p. 8723–8732.

Zhang, X., Lee, C. S. -M., Mingos, D. M. P. & Hayward, D. O., 2003. Carbon dioxide reforming of methane with Pt catalysts using microwave dielectric heating. *Catalysis Letters,* Volume 88, pp. 129-139.

APPENDICES

CO_2 and CH_4 Conversion graph calculation

Standard GC		
	Composition	Area
H_2	25.06	83.50318
CH_4	5.07	3211.841
CO_2	19.98	1.79E+04
N_2	-	-
CO	24.89	1.94E+04

Time (h)	Area CO_2			Area CH_4		
	1 wt%	3 wt%	5 wt%	1 wt%	3 wt%	5 wt%
0.5	1.80E+04	6275.58	3812.128	1.24E+04	4776.05	3601.703
1	1.47E+04	3765.51	3681.644	1.07E+04	3718.672	3559.115
1.5	1.85E+04	5407.766	3448.829	1.33E+04	5253.894	3335.962
2	1.80E+04	5355.922	4850.08	1.29E+04	5183.823	4658.293
2.5	1.79E+04	5498.002	5651.948	1.28E+04	5307.525	5357.468
3	1.80E+04	5512.188	4972.754	1.29E+04	5389.551	4747.877

Composition CO_2			Composition CH_4		
1 wt%	3 wt%	5 wt%	1 wt%	3 wt%	5 wt%
20.10175	7.015823	4.261791	19.54131	7.539158	5.685411
16.48706	4.209675	4.115917	16.88447	5.870051	5.618185
20.69437	6.045645	3.85564	21.0095	8.29345	5.26593
20.11315	5.987686	5.422177	20.32284	8.182842	7.353275
20.035	6.146525	6.31863	20.25796	8.37811	8.456947
20.14076	6.162384	5.559321	20.33704	8.50759	7.494687

Using $\frac{A_i}{A_s} = \frac{C_i}{C_s}$

where: A_i = area for each component. C_i = composition for each component

A_s = area for standard GC C_s = composition for standard GC

Flowrate CO_2 out			Flowrate CH_4 out		
1 wt%	3 wt%	5 wt%	1 wt%	3 wt%	5 wt%
9.508126	3.318484	2.015827	9.243038	3.566022	2.689199
7.798378	1.991176	1.946829	7.986357	2.776534	2.657401
9.788439	2.85959	1.823718	9.937494	3.922802	2.490785
9.513519	2.832176	2.56469	9.612702	3.870484	3.478099
9.476557	2.907306	2.988712	9.582015	3.962846	4.000136
9.52658	2.914808	2.629559	9.619422	4.02409	3.544987

$F_i = C_i$ x F_T

where: F_i = flowrate for each component. C_i = composition for each component

F_T = total flowrate (47.3 ml/m^3)

Conversion CO_2			Conversion CH_4		
1 wt%	3 wt%	5 wt%	1 wt%	3 wt%	5 wt%
19.71523	71.97936	82.97874	21.95358	69.8892	77.29292
34.152	83.18689	83.56136	32.56475	76.55549	77.56142
17.34832	75.85418	84.60088	16.08973	66.87662	78.96829
19.66968	76.08566	78.34426	18.8322	67.31838	70.6316
19.98179	75.45127	74.7639	19.09132	66.5385	66.22363
19.5594	75.38793	77.79652	18.77546	66.02136	70.06682

For conversion of CO_2

$X_{CO_2} = \left(\frac{F_{CO_2 in} - F_{CO_2 out}}{F_{CO_2 in}}\right)$ x 100

where:

$F_{CO_2 in}$ = 11.843 ml/m^3

For conversion of CH_4

$X_{CH_4} = \left(\frac{F_{CH_4 in} - F_{CH_4 out}}{F_{CH_4 in}}\right)$ x 100

where:

$F_{CH_4 in}$ = 11.843 ml/m^3

Yield of H_2 graph calculation

Area H_2			Composition H_2		
1 wt%	3 wt%	5 wt%	1 wt%	3 wt%	5 wt%
0	5.404	5.409	0	1.621785	1.623286
1.71753	5.405	5.41	0.515445	1.622086	1.623586
2.10952	5.409	5.407	0.633085	1.623286	1.622686
1.4494	5.408	5.28	0.434977	1.622986	1.584572
1.194	5.409	5.33	0.358329	1.623286	1.599577
1.47486	5.41	5.32	0.442618	1.623586	1.596576

Using $\frac{A_i}{A_s} = \frac{C_i}{C_s}$

where: A_i = area for each component. C_i = composition for each component

A_s = area for standard GC C_s = composition for standard GC

Flowrate H_2 out			Yeild H_2		
1 wt%	3 wt%	5 wt%	1 wt%	3 wt%	5 wt%
0	0.767105	0.767814	0	3.238641	3.241638
0.243806	0.767246	0.767956	1.029323	3.23924	3.242237
0.299449	0.767814	0.76753	1.264245	3.241638	3.240439
0.205744	0.767672	0.749503	0.868632	3.241038	3.164327
0.16949	0.767814	0.7566	0.715569	3.241638	3.194292
0.209358	0.767956	0.755181	0.88389	3.242237	3.188299

$F_i = C_i$ x F_T

where: F_i = flowrate for each component. C_i = composition for each component

F_T = total flowrate (47.3 ml/m^3)

For yield of H_2

$Y_{H_2} = \left(\frac{F_{H_2 out}}{2 \text{ x } F_{CH_4 in}}\right)$ x 100

FKKSA CONSULTATION & SERVICES UNIT
Universiti Malaysia Pahang (UMP)
Lebuhraya Tun Razak, Gambang
26300 Kuantan
Pahang Darul Makmur
Tel : 09-549 2841 / 09-549 2803 | Fax : 09-549 3383
Email : mahadhir@ump.edu.my

CERTIFICATE OF ANALYSIS

To :	Mohamad Irsyad (KA 11076)		Attn :	
Address :	Fakulti Kejuruteraan Kimia Dan Sumber Asli (FKKSA) Universiti Malaysia Pahang			
c.c. :			Total Page :	2
Tel No :	017-929 1225	Fax No :	Date :	04/06/2015

Sample Description : BLANK-R10-21052015
Date Sample Receive : 14/05/2015
Date Reported : 04/06/2015

RESULT

Sample Properties

Sample Tag :	BLANK
Sample Weight :	5.5520mg
Method :	Ramp 10°C/min
	max Temp = 900°C
Sample purge :	N_2 (40ml/min)
Balance purge :	N_2 (60ml/min)
Date :	21/05/2015

TGA Result Analysis

Material	Composition	Tem.Decomp
	%	°C
1	10.07	N/A
2	1.609	213.17
3	3.612	327.67
4	N/A	N/A
Residue	84.20	at 900

Notes :

Highly Volatile Matter

*moisture, plasticizer, residual solvent and other low boiling components <200°C to 300°C

Medium Volatile Matter

*oil, polymer degradation products that volatilise in the range 200°C to 700°C

Combustible material

*Oxidizable matter that do not volatilise at 750oC or some specified temperature depend on material

Ash

*Non-volatile residues in an oxidizing atmosphere. Metal components, fillers or inert reinforcing agents

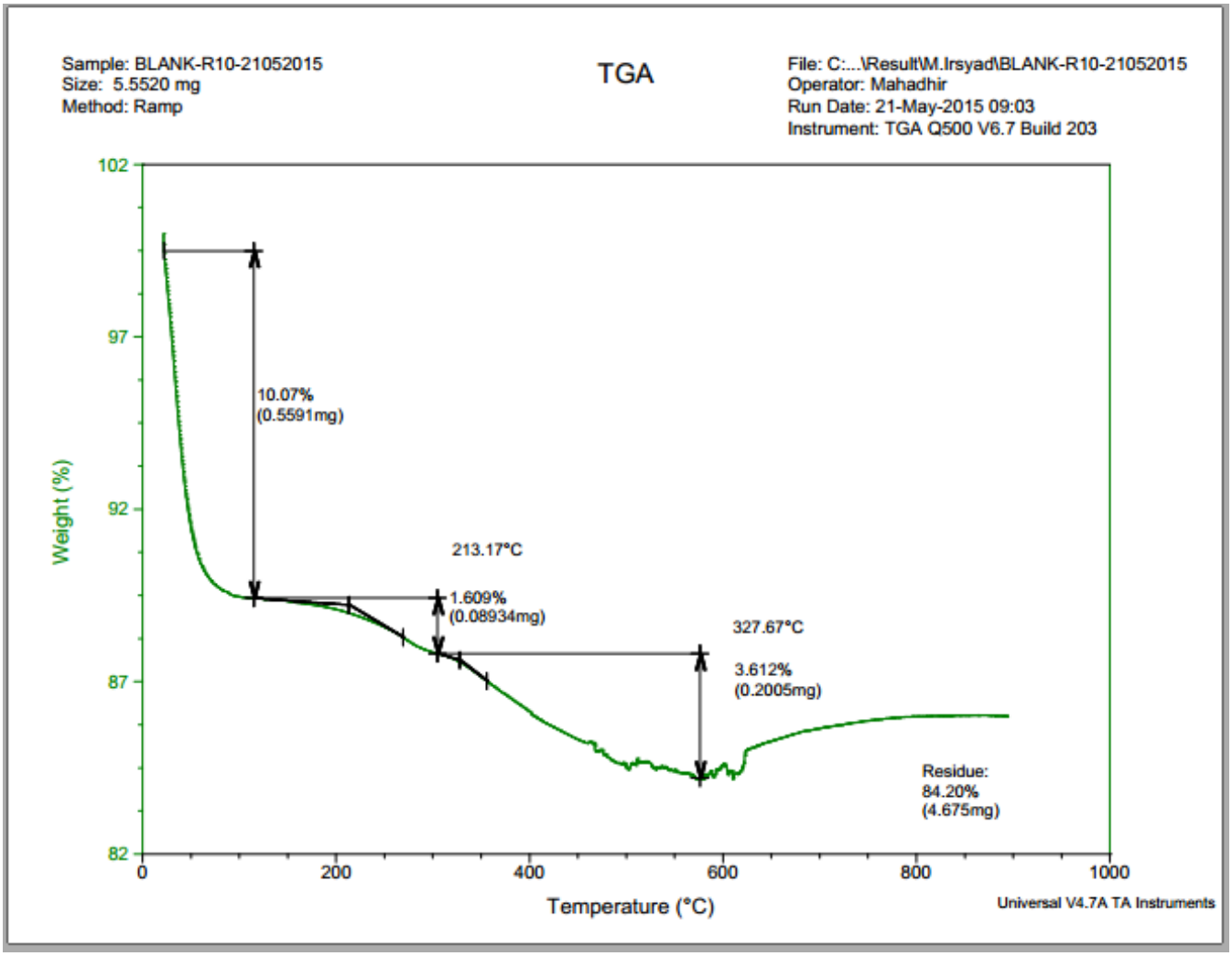

FKKSA CONSULTATION & SERVICES UNIT
Universiti Malaysia Pahang (UMP)
Lebuhraya Tun Razak, Gambang
26300 Kuantan
Pahang Darul Makmur
Tel : 09-549 2841 / 09-549 2803 | Fax : 09-549 3383
Email : mahadhir@ump.edu.my

CERTIFICATE OF ANALYSIS

To :	Mohamad Irsyad (KA 11076)	Attn :	
Address :	Fakulti Kejuruteraan Kimia Dan Sumber Asli (FKKSA) Universiti Malaysia Pahang		
c.c. :		Total Page :	2
Tel No :	017-929 1225 Fax No :	Date :	04/06/2015

Sample Description : 1wt%-R10-03062015
Date Sample Receive : 14/05/2015
Date Reported : 04/06/2015

RESULT

Sample Properties

Sample Tag :	1wt%
Sample Weight :	4.8850mg
Method :	Ramp 10°C/min
	max Temp = 900°C
Sample purge :	N_2 (40ml/min)
Balance purge :	N_2 (60ml/min)
Date :	03/06/2015

TGA Result Analysis

Material	Composition	Tem.Decomp
	%	°C
1	3.192	N/A
2	2.066	220.74
3	3.561	341.74
4	N/A	N/A
Residue	90.91	at 900

Notes :

Highly Volatile Matter

*moisture, plasticizer, residual solvent and other low boiling components <200^{o}C to 300^{o}C

Medium Volatile Matter

*oil, polymer degradation products that volatilise in the range 200^{o}C to 700^{o}C

Combustible material

*Oxidizable matter that do not volatilise at 750oC or some specified temperature depend on material

Ash

*Non-volatile residues in an oxidizing atmosphere. Metal components, fillers or inert reinforcing agents

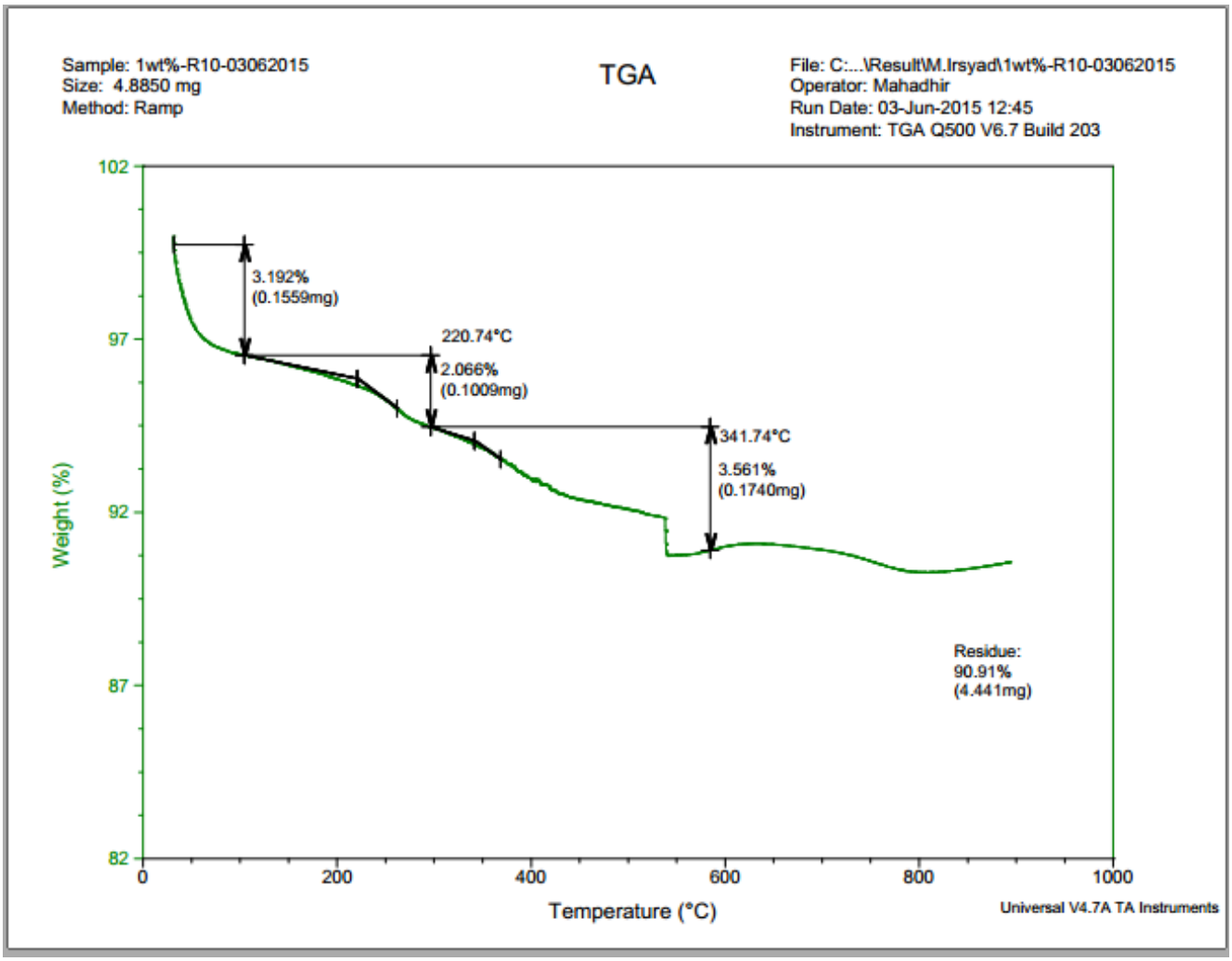

FKKSA CONSULTATION & SERVICES UNIT
Universiti Malaysia Pahang (UMP)
Lebuhraya Tun Razak, Gambang
26300 Kuantan
Pahang Darul Makmur
Tel : 09-549 2841 / 09-549 2803 | Fax : 09-549 3383
Email : mahadhir@ump.edu.my

CERTIFICATE OF ANALYSIS

To :	Mohamad Irsyad (KA 11076)	Attn :	
Address :	Fakulti Kejuruteraan Kimia Dan Sumber Asli (FKKSA) Universiti Malaysia Pahang		
c.c. :		Total Page :	2
Tel No :	017-929 1225 Fax No :	Date :	04/06/2015

Sample Description : 3wt%-R10-03062015
Date Sample Receive : 14/05/2015
Date Reported : 04/06/2015

RESULT

Sample Properties

Sample Tag :	3wt%
Sample Weight :	5.2430mg
Method :	Ramp 10°C/min
	max Temp = 900°C
Sample purge :	N_2 (40ml/min)
Balance purge :	N_2 (60ml/min)
Date :	03/06/2015

TGA Result Analysis

Material	Composition	Tem.Decomp
	%	°C
1	5.452	N/A
2	1.466	235.48
3	2.791	345.33
4	N/A	N/A
Residue	90.28	at 900

Notes :

Highly Volatile Matter

*moisture, plasticizer, residual solvent and other low boiling components <200^{o}C to 300^{o}C

Medium Volatile Matter

*oil, polymer degradation products that volatilise in the range 200^{o}C to 700^{o}C

Combustible material

*Oxidizable matter that do not volatilise at 750oC or some specified temperature depend on material

Ash

*Non-volatile residues in an oxidizing atmosphere. Metal components, fillers or inert reinforcing agents

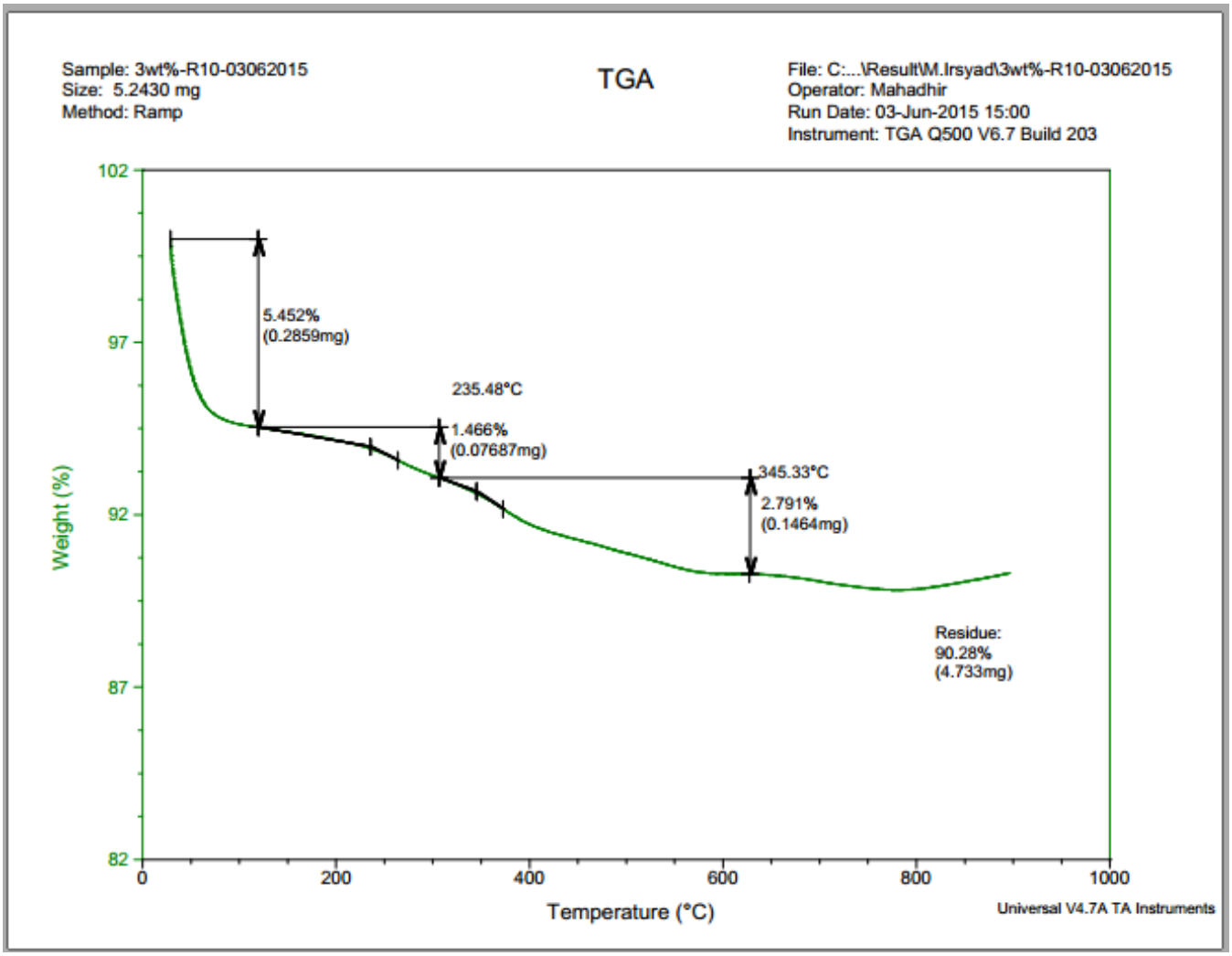

FKKSA CONSULTATION & SERVICES UNIT
Universiti Malaysia Pahang (UMP)
Lebuhraya Tun Razak, Gambang
26300 Kuantan
Pahang Darul Makmur
Tel : 09-549 2841 / 09-549 2803 | Fax : 09-549 3383
Email : mahadhir@ump.edu.my

CERTIFICATE OF ANALYSIS

To :	Mohamad Irsyad (KA 11076)	Attn :	
Address :	Fakulti Kejuruteraan Kimia Dan Sumber Asli (FKKSA) Universiti Malaysia Pahang		
c.c. :		Total Page :	2
Tel No :	017-929 1225 Fax No :	Date :	04/06/2015

Sample Description : 5wt%-R10-04062015
Date Sample Receive : 14/05/2015
Date Reported : 04/06/2015

RESULT

Sample Properties

Sample Tag :	5wt%
Sample Weight :	5.9350mg
Method :	Ramp 10°C/min
	max Temp = 900°C
Sample purge :	N_2 (40ml/min)
Balance purge :	N_2 (60ml/min)
Date :	04/06/2015

TGA Result Analysis

Material	Composition	Tem.Decomp
	%	°C
1	8.955	N/A
2	0.9622	231.62
3	2.059	334.84
4	N/A	N/A
Residue	87.91	at 900

Notes :

Highly Volatile Matter

*moisture, plasticizer, residual solvent and other low boiling components <200^{o}C to 300^{o}C

Medium Volatile Matter

*oil, polymer degradation products that volatilise in the range 200^{o}C to 700^{o}C

Combustible material

*Oxidizable matter that do not volatilise at 750oC or some specified temperature depend on material

Ash

*Non-volatile residues in an oxidizing atmosphere. Metal components, fillers or inert reinforcing agents

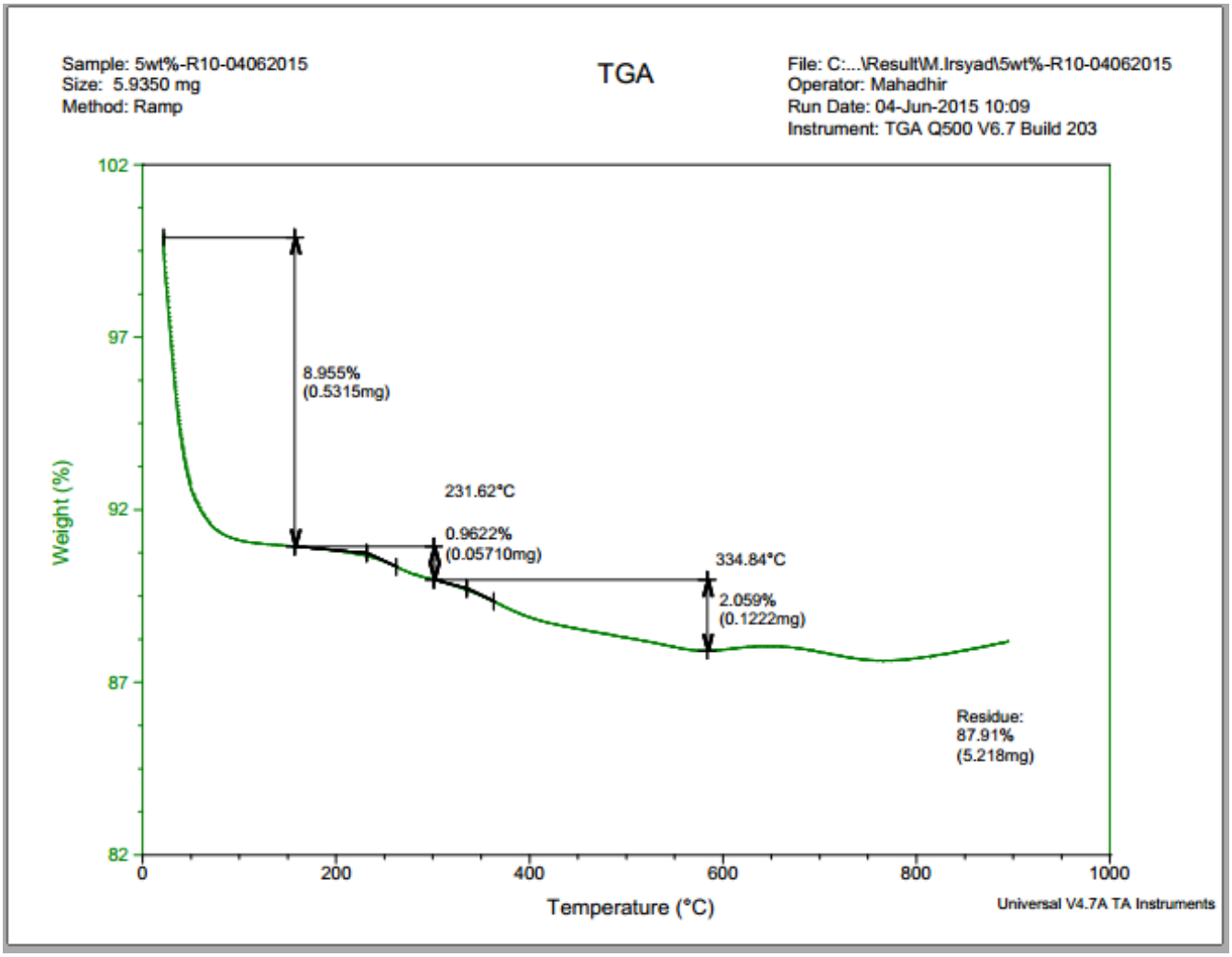

XRD Analysis Results

General Information

Analysis date	5/26/2015 2:45:01 PM		
Sample name	XRD Analysis	Measured time	5/22/2015 9:37:34 AM
File name	SBA 15.raw	Operator	administrator
Comment	UMP		

Measurement profile

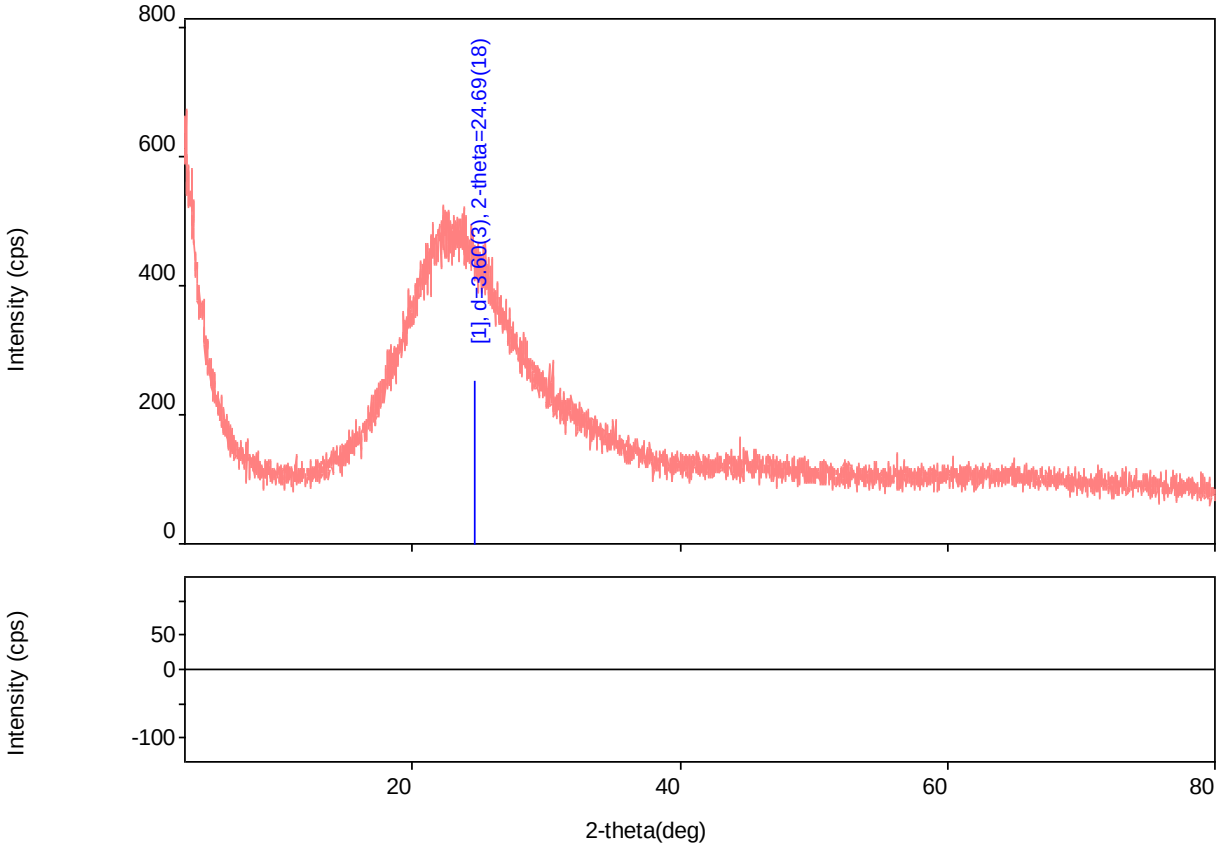
800
600
400
200
0
Intensity (cps)
[1], d=3.60(3), 2-theta=24.69(18)
50
0
-100
Intensity (cps)
20
40
60
80
2-theta(deg)

Measurement conditions

XG	Cu/30 kV/15 mA	Duration time / Scan speed	1 deg/min
Goniometer		Step / Sampling step	0.02 deg
Attachment	-	Measurement axis	2ƒÆ/ƒÆ
K-beta filter	-	Scan range	3-80 deg
Incident monochromator	-	Incident slit	-
Receiving monochromator	-	Vertical divergence slit	-
Counter	-	Receiving slit #1	-
		Receiving slit #2	-

Qualitative analysis results

Phase name	Formula	Figure of merit	ICDD
Graphite-2H	C	0.2648115493404479	411487 (ICDD)

Phase name	Formula	Space group	ICDD
Graphite-2H	C	194 : P63/mmc	411487 (ICDD)

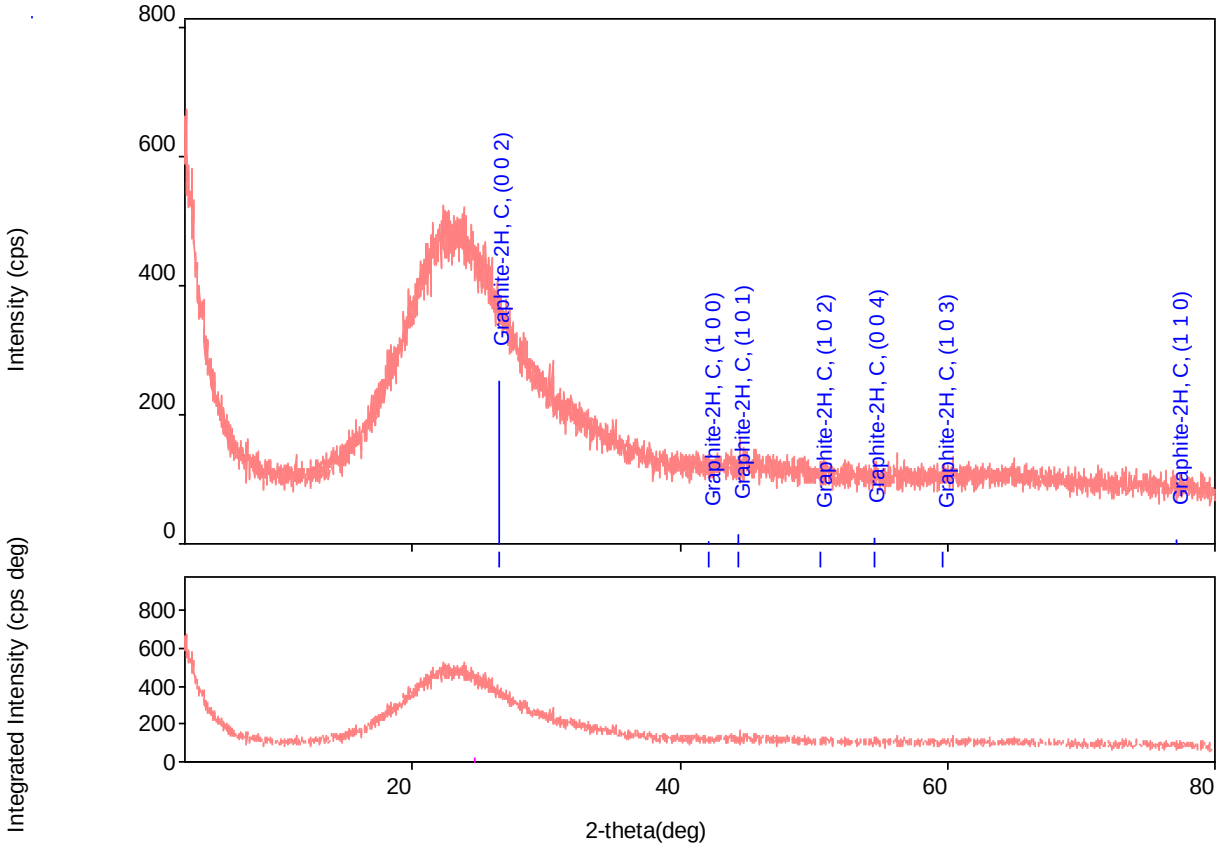
Intensity (cps)
800
600
400
200
0
Graphite-2H, C, (0 0 2)
Graphite-2H, C, (1 0 0)
Graphite-2H, C, (1 0 1)
Graphite-2H, C, (1 0 2)
Graphite-2H, C, (0 0 4)
Graphite-2H, C, (1 0 3)
Graphite-2H, C, (1 1 0)
Integrated Intensity (cps deg)
800
600
400
200
0
20
40
60
80
2-theta(deg)

Peak list

2-theta (deg)	d (ang.)	Height (cps)	Int. I(cps¥deg)	FWHM(deg)	Size	Phase name
24.69(18)	3.60(3)	255(16)	2901(138)	8.22(18)	10.3(2)	Graphite-2H, (0,0,2)

XRD Analysis Results

General Information

Analysis date	5/26/2015 2:38:51 PM		
Sample name	XRD Analysis	Measured time	5/22/2015 10:47:26 AM
File name	1wt%.raw	Operator	administrator
Comment	UMP		

Measurement profile

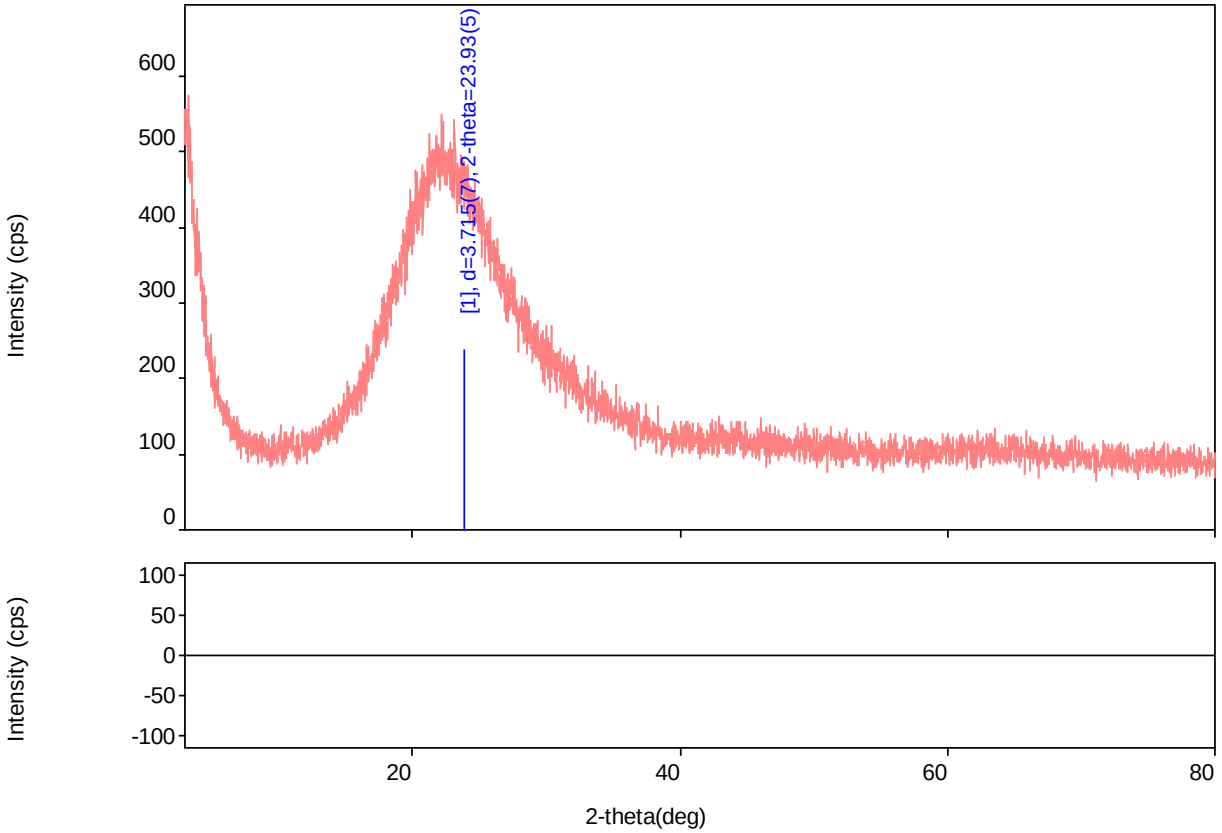
600
500
400
300
200
100
0
Intensity (cps)
[1], d=3.715(7), 2-theta=23.93(5)
100
50
0
-50
-100
Intensity (cps)
20
40
60
80
2-theta(deg)

Measurement conditions

XG	Cu/30 kV/15 mA	Duration time / Scan speed	1 deg/min
Goniometer		Step / Sampling step	0.02 deg
Attachment	-	Measurement axis	2ƒÆ/ƒÆ
K-beta filter	-	Scan range	3-80 deg
Incident monochromator	-	Incident slit	-
Receiving monochromator	-	Vertical divergence slit	-
Counter	-	Receiving slit #1	-
		Receiving slit #2	-

Qualitative analysis results

Phase name	Formula	Figure of merit	ICDD
Graphite-2H	C	0.285308954275647	411487 (ICDD)

Phase name	Formula	Space group	ICDD
Graphite-2H	C	194 : P63/mmc	411487 (ICDD)

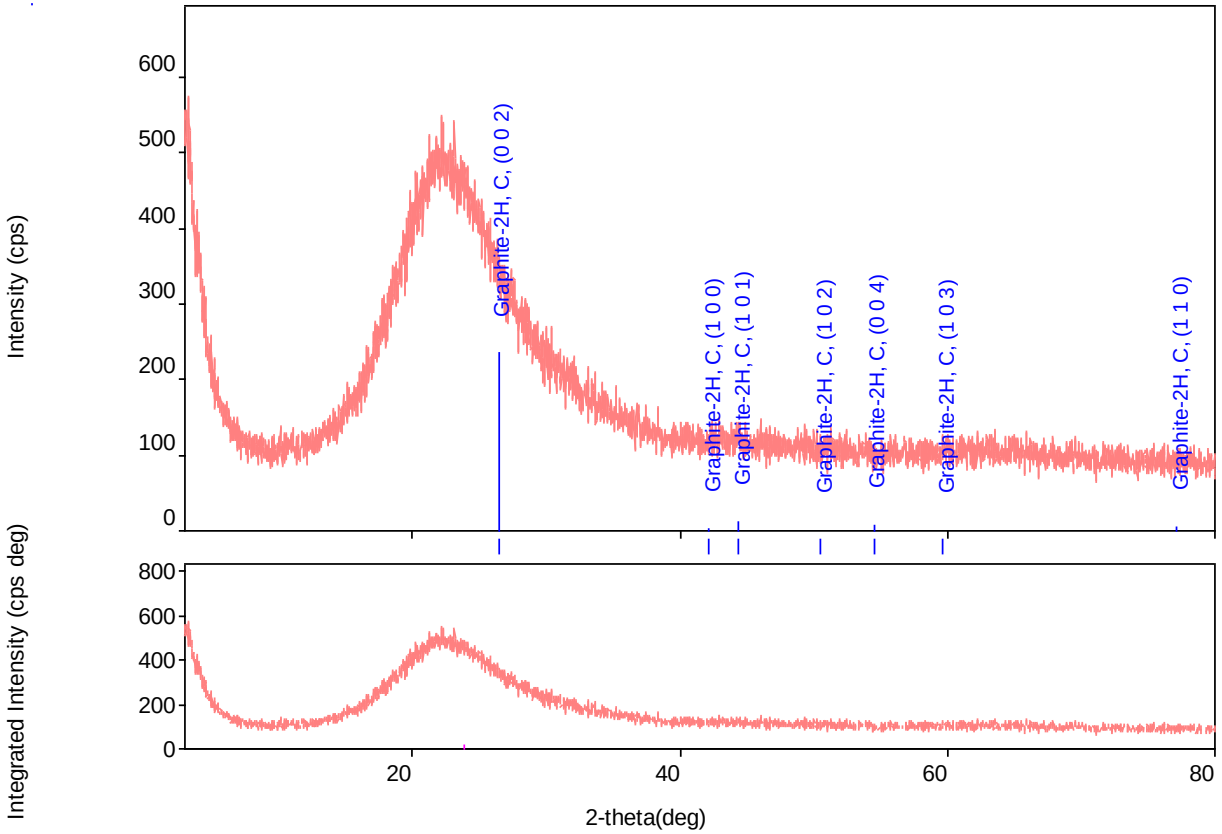
Intensity (cps)
600
500
400
300
200
100
0
Graphite-2H, C, (0 0 2)
Graphite-2H, C, (1 0 0)
Graphite-2H, C, (1 0 1)
Graphite-2H, C, (1 0 2)
Graphite-2H, C, (0 0 4)
Graphite-2H, C, (1 0 3)
Graphite-2H, C, (1 1 0)
Integrated Intensity (cps deg)
800
600
400
200
0
20
40
60
80
2-theta(deg)

Peak list

2-theta (deg)	d (ang.)	Height (cps)	Int. I(cps¥deg)	FWHM(deg)	Size	Phase name
23.93(5)	3.715(7)	239(15)	2644(42)	8.71(14)	9.73(15)	Graphite-2H, (0,0,2)

XRD Analysis Results

General Information

Analysis date	5/26/2015 2:41:24 PM		
Sample name	XRD Analysis	Measured time	5/22/2015 1:03:40 PM
File name	3wt%.raw	Operator	administrator
Comment	UMP		

Measurement profile

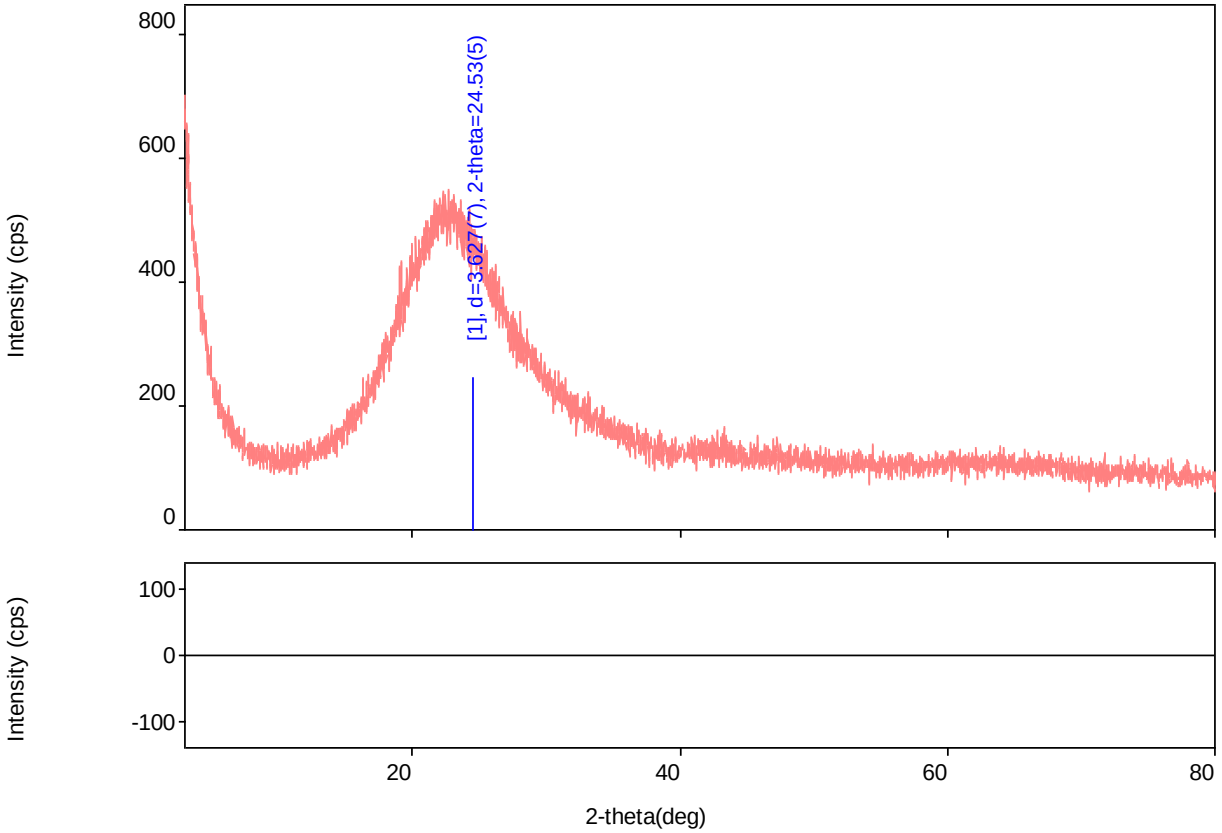
800
600
400
200
0
Intensity (cps)
[1], d=3.627(7), 2-theta=24.53(5)
100
0
-100
Intensity (cps)
20
40
60
80
2-theta(deg)

Measurement conditions

XG	Cu/30 kV/15 mA	Duration time / Scan speed	1 deg/min
Goniometer		Step / Sampling step	0.02 deg
Attachment	-	Measurement axis	2ƒÆ/ƒÆ
K-beta filter	-	Scan range	3-80 deg
Incident monochromator	-	Incident slit	-
Receiving monochromator	-	Vertical divergence slit	-
Counter	-	Receiving slit #1	-
		Receiving slit #2	-

Qualitative analysis results

Phase name	Formula	Figure of merit	ICDD
Graphite-2H	C	0.2671185450915248	411487 (ICDD)

Phase name	Formula	Space group	ICDD
Graphite-2H	C	194 : P63/mmc	411487 (ICDD)

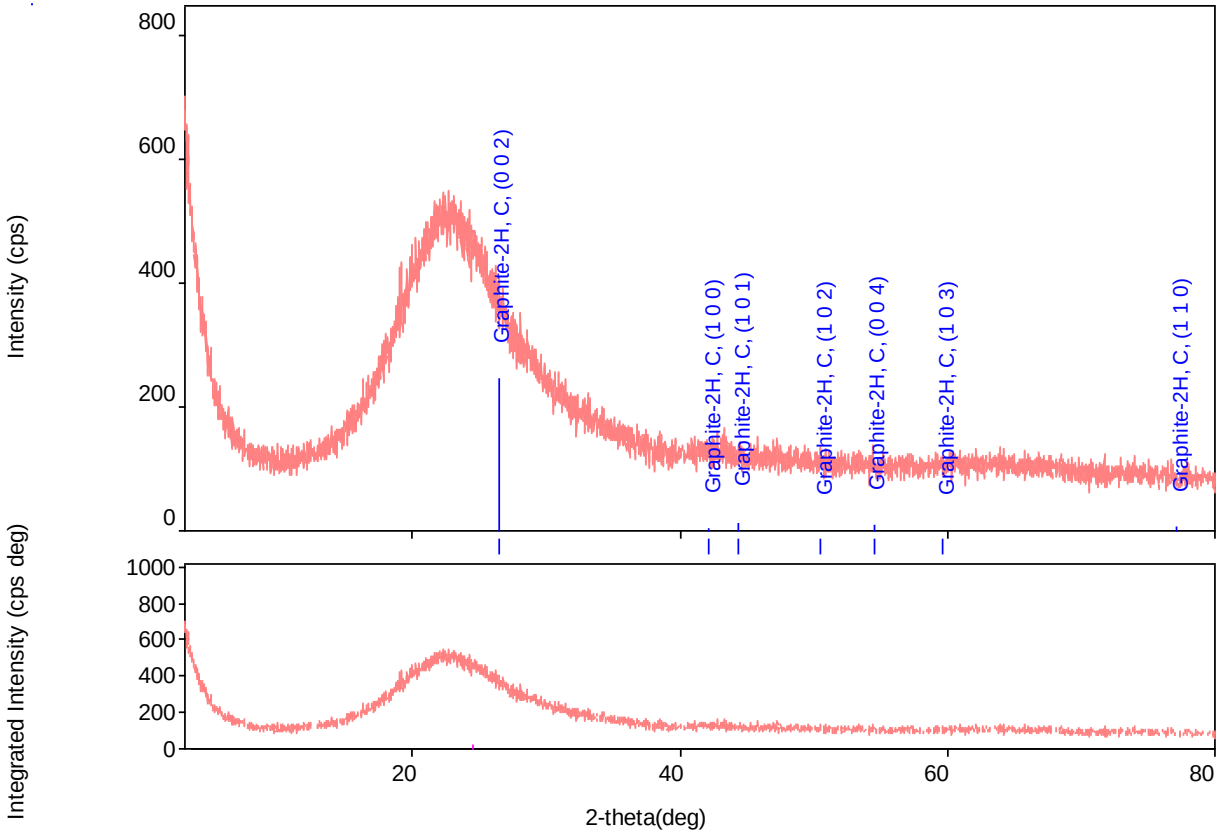
Intensity (cps)
800
600
400
200
0
Graphite-2H, C, (0 0 2)
Graphite-2H, C, (1 0 0)
Graphite-2H, C, (1 0 1)
Graphite-2H, C, (1 0 2)
Graphite-2H, C, (0 0 4)
Graphite-2H, C, (1 0 3)
Graphite-2H, C, (1 1 0)
Integrated Intensity (cps deg)
1000
800
600
400
200
0
20
40
60
80
2-theta(deg)

Peak list

2-theta (deg)	d (ang.)	Height (cps)	Int. I(cps¥deg)	FWHM(deg)	Size	Phase name
24.53(5)	3.627(7)	249(16)	2722(44)	8.61(15)	9.86(17)	Graphite-2H, (0,0,2)

XRD Analysis Results

General Information

Analysis date	5/26/2015 2:43:41 PM		
Sample name	XRD Analysis	Measured time	5/22/2015 11:55:30 AM
File name	5wt%.raw	Operator	administrator
Comment	UMP		

Measurement profile

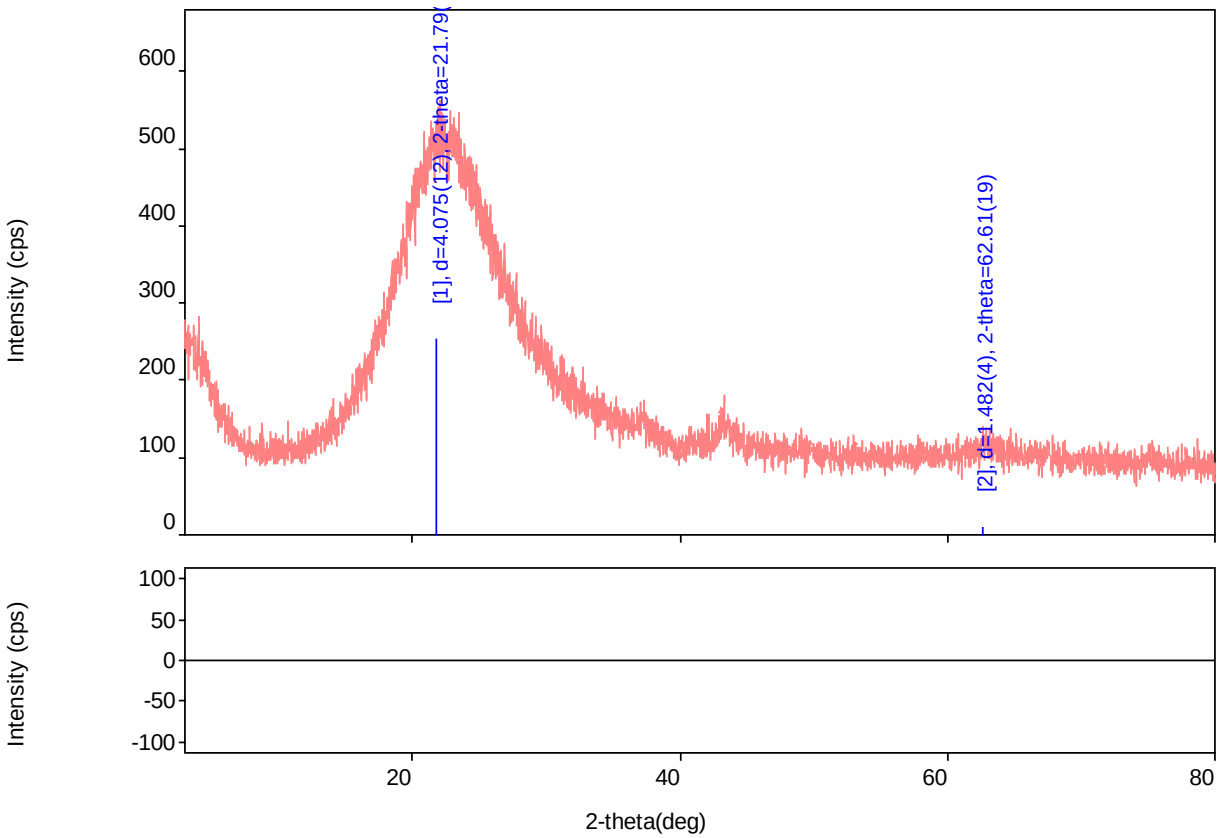
Intensity (cps)
600
500
400
300
200
100
0
[1], d=4.075(12), 2-theta=21.79(
[2], d=1.482(4), 2-theta=62.61(19)
Intensity (cps)
100
50
0
-50
-100
20
40
60
80
2-theta(deg)

Measurement conditions

XG	Cu/30 kV/15 mA	Duration time / Scan speed	1 deg/min
Goniometer		Step / Sampling step	0.02 deg
Attachment	-	Measurement axis	2ƒÆ/ƒÆ
K-beta filter	-	Scan range	3-80 deg
Incident monochromator	-	Incident slit	-
Receiving monochromator	-	Vertical divergence slit	-
Counter	-	Receiving slit #1	-
		Receiving slit #2	-

Qualitative analysis results

Phase name	Formula	Figure of merit	ICDD
Graphite-2H	C	0.437525060590793	411487 (ICDD)

Phase name	Formula	Space group	ICDD
Graphite-2H	C	194 : P63/mmc	411487 (ICDD)

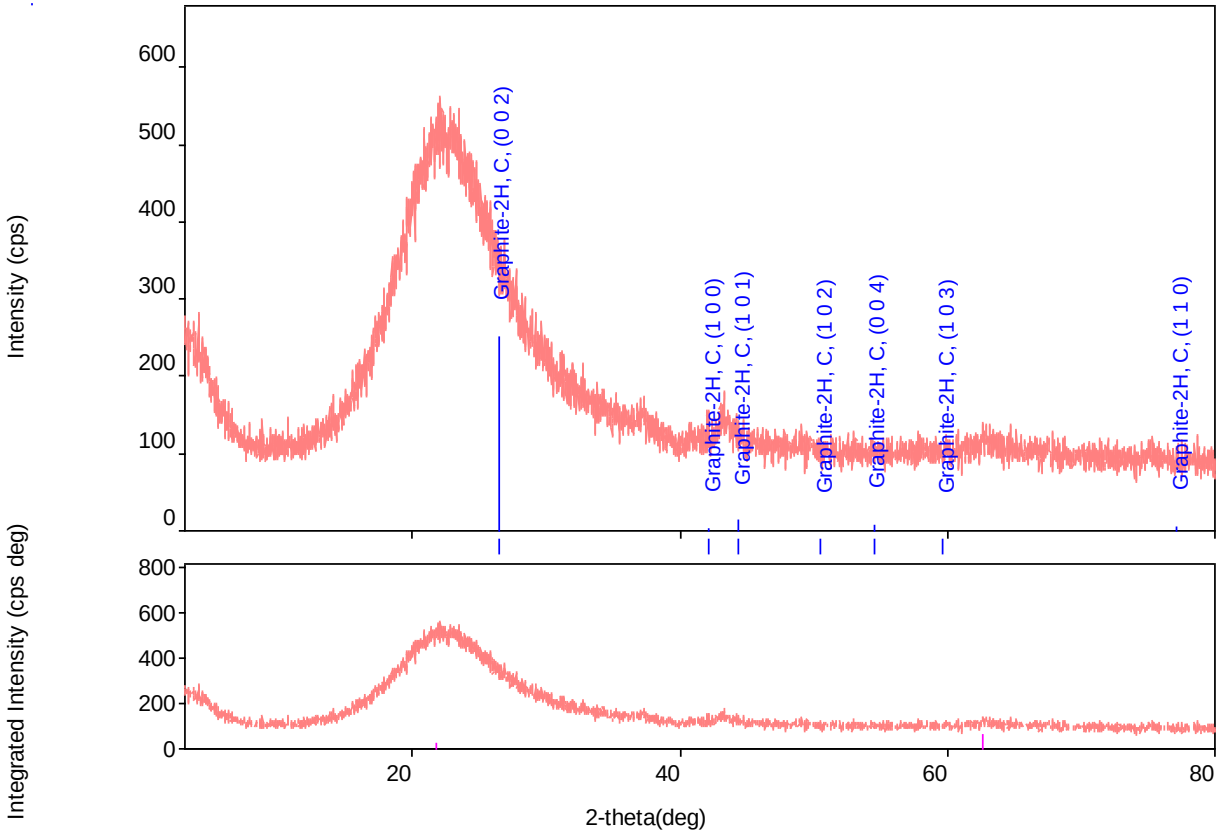
Intensity (cps)
600
500
400
300
200
100
0
Graphite-2H, C, (0 0 2)
Graphite-2H, C, (1 0 0)
Graphite-2H, C, (1 0 1)
Graphite-2H, C, (1 0 2)
Graphite-2H, C, (0 0 4)
Graphite-2H, C, (1 0 3)
Graphite-2H, C, (1 1 0)
Integrated Intensity (cps deg)
800
600
400
200
0
20
40
60
80
2-theta(deg)

Peak list

2-theta (deg)	d (ang.)	Height (cps)	Int. I(cps¥deg)	FWHM(deg)	Size	Phase name
21.79(6)	4.075(12)	255(16)	2864(18)	9.07(7)	9.31(7)	Graphite-2H, (0,0,2)
62.61(19)	1.482(4)	11(3)	45(4)	2.6(3)	37(5)	Unknown,

BET Analysis Result

Ni/SBA-15

Isotherm

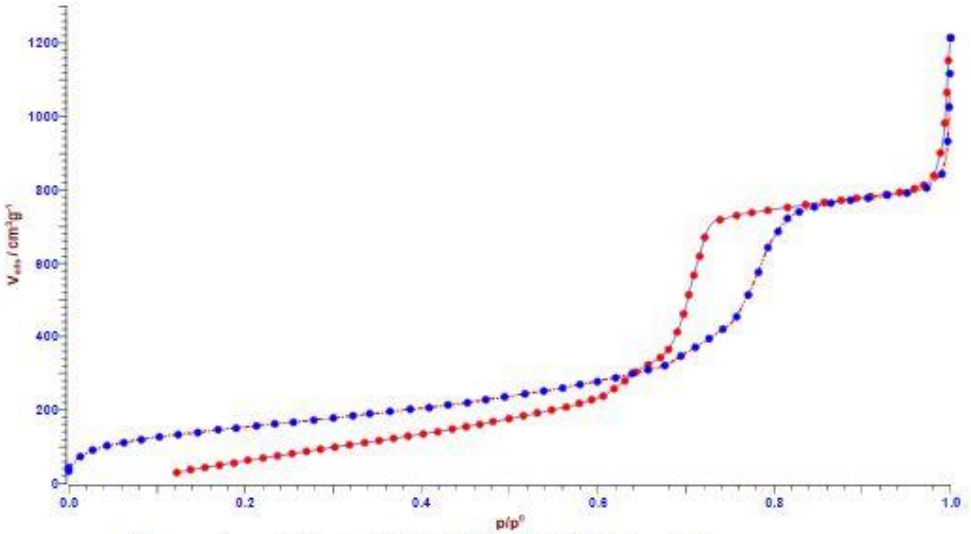

Pore volume (Gurvich) at p/p^0 0.95 is 1.2241 cm^3g^{-1}

Surface Area (Langmuir)

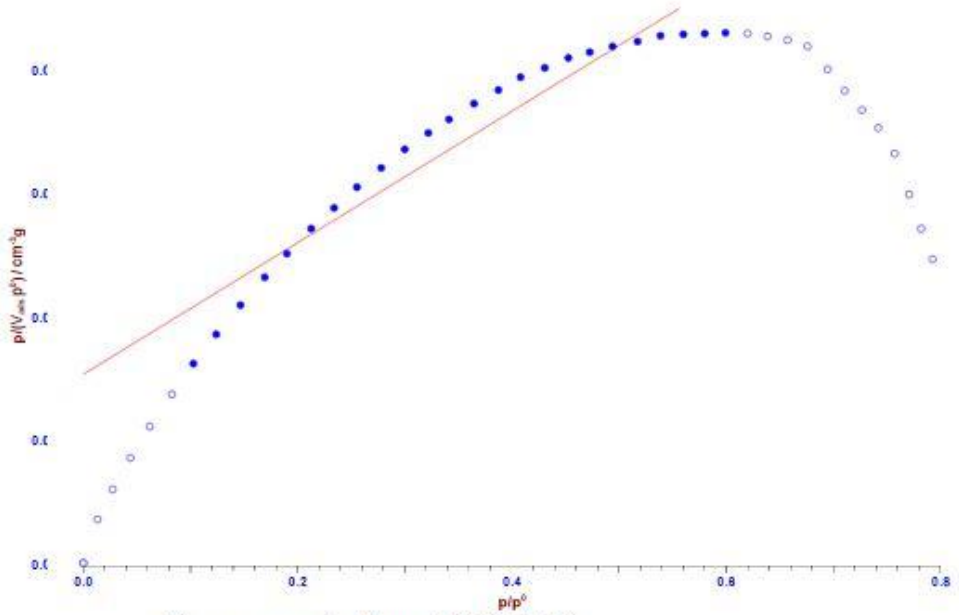

Linear regression from p/p^0	0.1 to 0.6
Offset:	0.00076763 ± 6.18675E-5
Slope:	0.00266804 ± 0.00016112
R:	0.9621478
Monoloayer volume	374.81 cm^3g^{-1}
Monoloayer amount:	16.722 mmol g^{-1}
B:	3.4757
Calculation with a molecular area of	16.2 $Å^2$
Surface area was:	1631.4 m^2g^{-1}

Mesopores (B.J.H.)

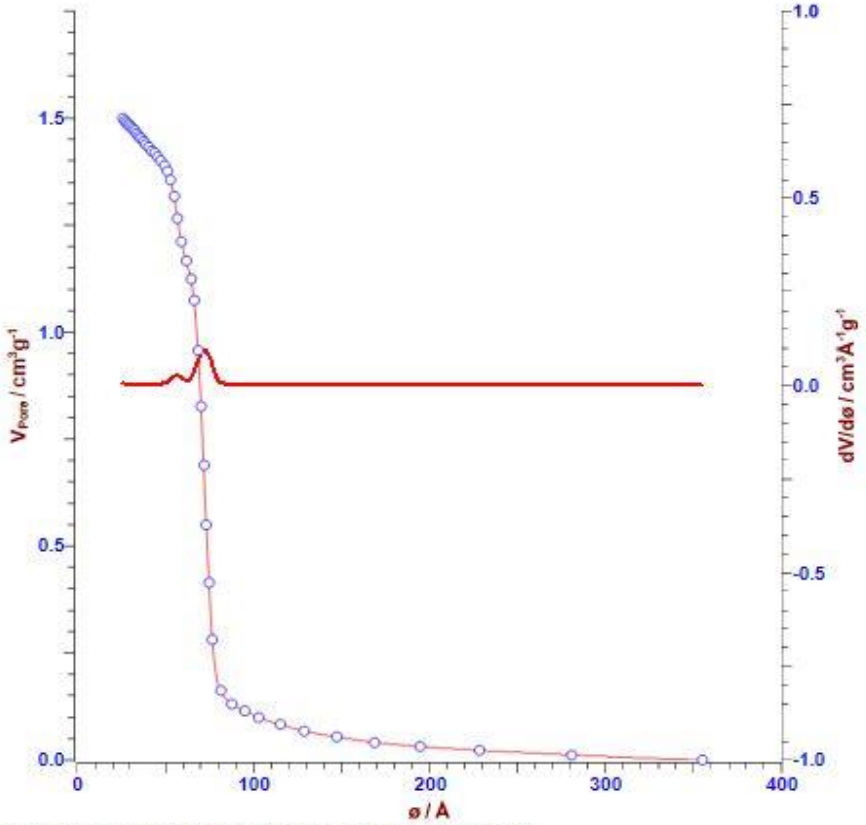

Calculations used Desorption Branch from p/p^0 0.3 to 0.95
with standard isotherm: Universal (Harkins,Jura)
from literature: ASTM Standards Designation: D 4641-87

Calculation with a molecular area of	16.2 $Å^2$
molecular weight of	28.01 g/mol
liquid density of	0.8086 g cm^{-3}
and surface tension of	8.85 Dyne cm^{-1}
Median pore diameter	71.17 Å
Maximum pore diameter	72.022 Å
Cumulative pore volume	1.5002 cm^3g^{-1}
Cumulative pore area	894.31 m^2g^{-1}

1% Ni/SBA-15

Isotherm

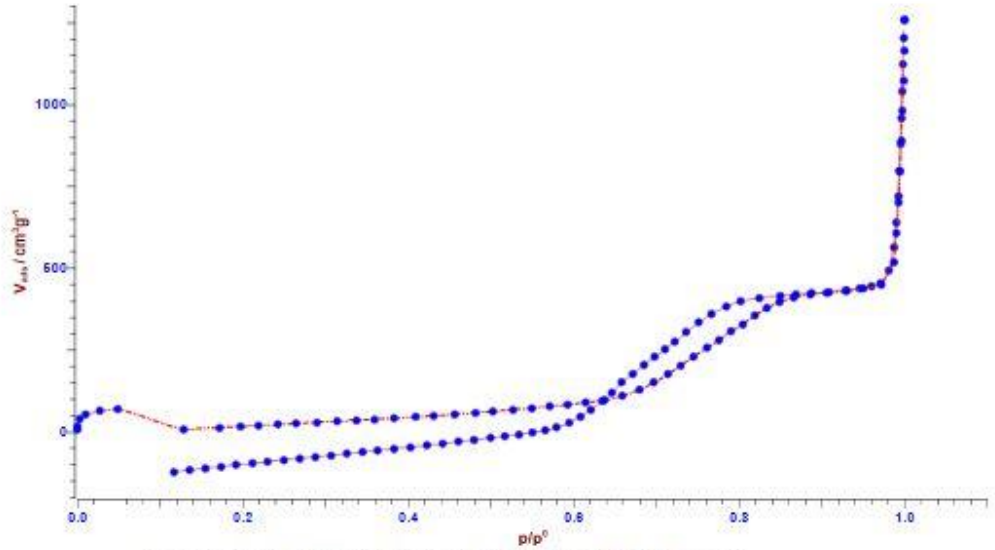

Pore volume (Gurvich) at p/p^0 0.95 is 0.6771 cm^3g^{-1}

Surface Area (Langmuir)

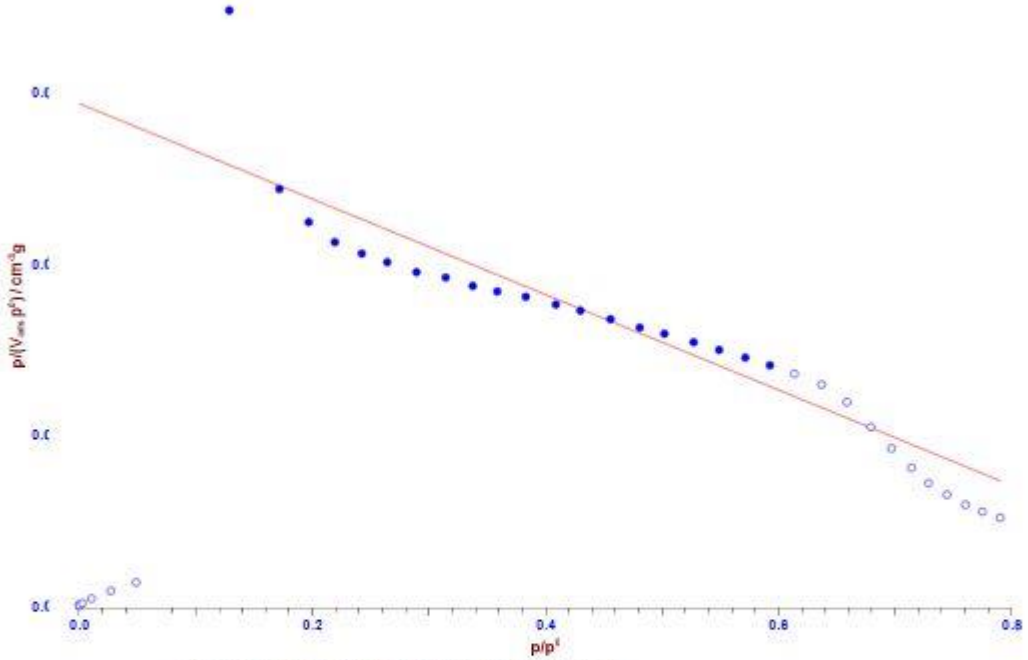

Linear regression from p/p^0 0.1 to 0.6

Offset: 0.01468803 ± 0.0007903
Slope: -0.0139685 ± 0.0019964
R: -0.8550818

Monoloayer volume -71.59 cm^3g^{-1}
Monoloayer amount: -3.194 mmol g^{-1}
B: -0.951

Calculation with a molecular area of 16.2 $Å^2$
Surface area was: -311.6 m^2g^{-1}

Mesopores (B.J.H.)

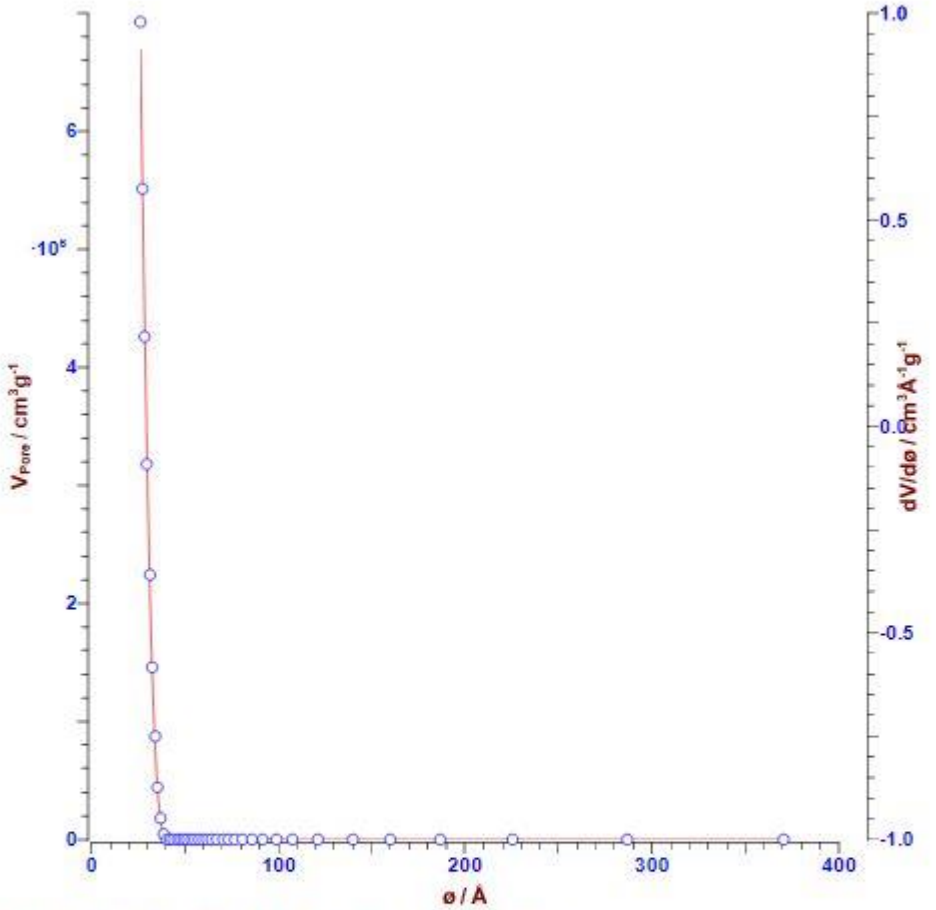

Calculations used Desorption Branch from p/p^0 0.3 to 0.95
with standard isotherm: Universal (Harkins,Jura)
from literature: ASTM Standards Designation: D 4641-87

Calculation with a molecular area of	16.2 Å²
molecular weight of	28.01 g/mol
liquid density of	0.8086 g cm⁻³
and surface tension of	8.85 Dyne cm⁻¹
Median pore diameter	68.312 Å
Maximum pore diameter	26.294 Å
Cumulative pore volume	1.0622 cm³g⁻¹
Cumulative pore area	610.14 m²g⁻¹

3% Ni/SBA-15

Isotherm

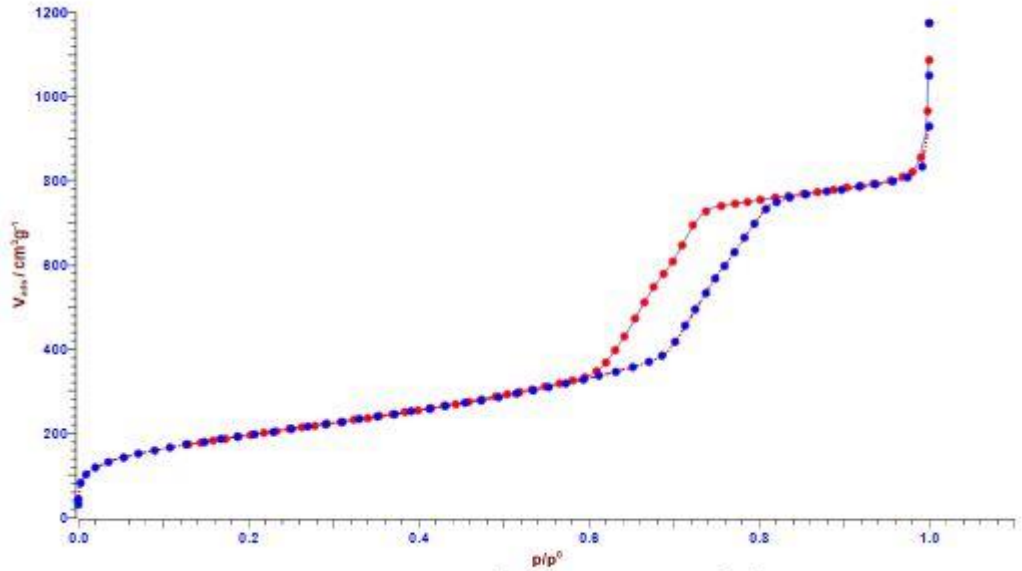

Pore volume (Gurvich) at p/p^0 0.95 is 1.2298 cm^3g^{-1}

Surface Area (Langmuir)

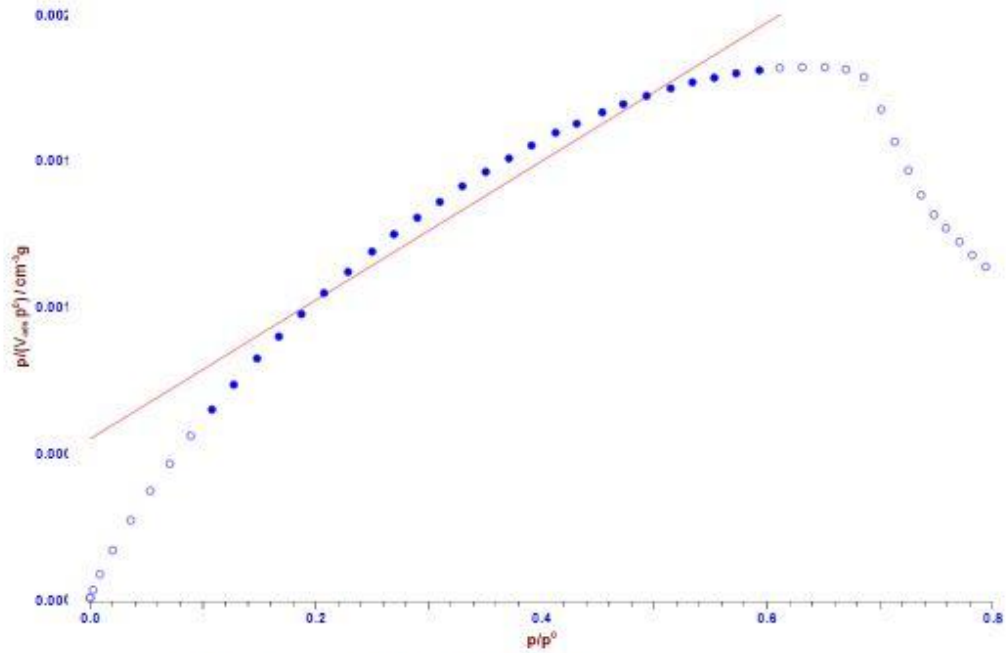

Linear regression from p/p^0 0.1 to 0.6

Offset: 0.00054731 ± 4.06248E-5

Slope: 0.00237372 ± 0.00010686

R: 0.97747714

Monoloayer volume 421.28 cm^3g^{-1}

Monoloayer amount: 18.796 mmol g^{-1}

B: 4.3371

Calculation with a molecular area of 16.2 $Å^2$

Surface area was: 1833.7 m^2g^{-1}

Mesopores (B.J.H.)

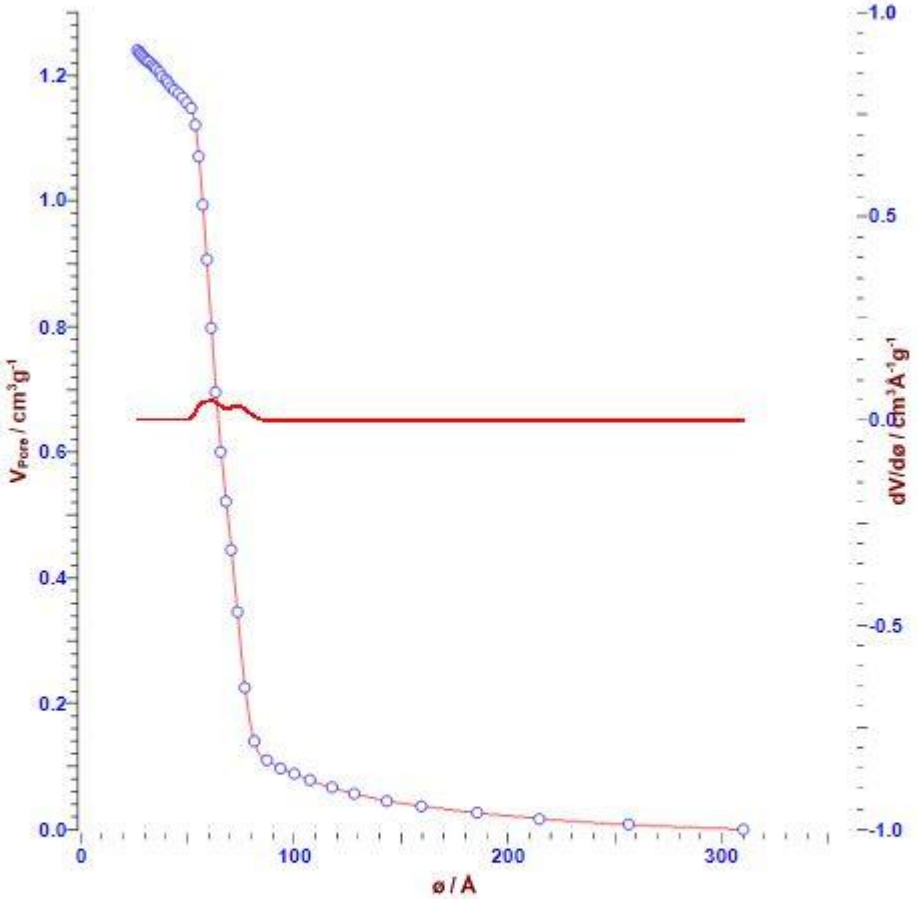

Calculations used Desorption Branch from p/p^0 0.3 to 0.95
with standard isotherm: Universal (Harkins,Jura)
from literature: ASTM Standards Designation: D 4641-87

Calculation with a molecular area of	16.2 Å²
molecular weight of	28.01 g/mol
liquid density of	0.8086 g cm^{-3}
and surface tension of	8.85 Dyne cm^{-1}
Median pore diameter	64.974 Å
Maximum pore diameter	60.9 Å
Cumulative pore volume	1.2401 cm^3g^{-1}
Cumulative pore area	769.69 m^2g^{-1}

5% Ni/SBA-15

Isotherm

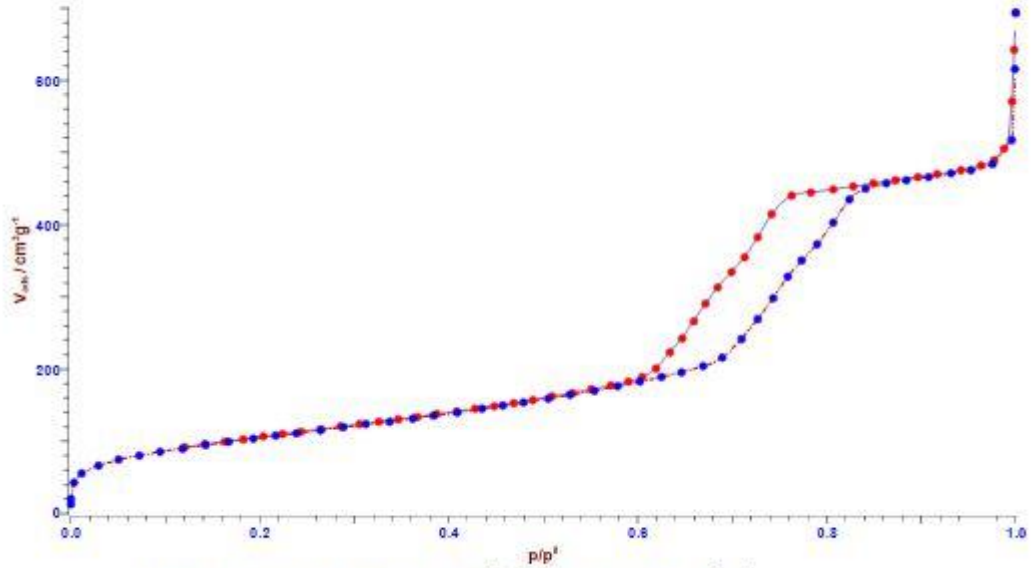

Pore volume (Gurvich) at p/p^0 0.95 is 0.734 cm^3g^{-1}

Surface Area (Langmuir)

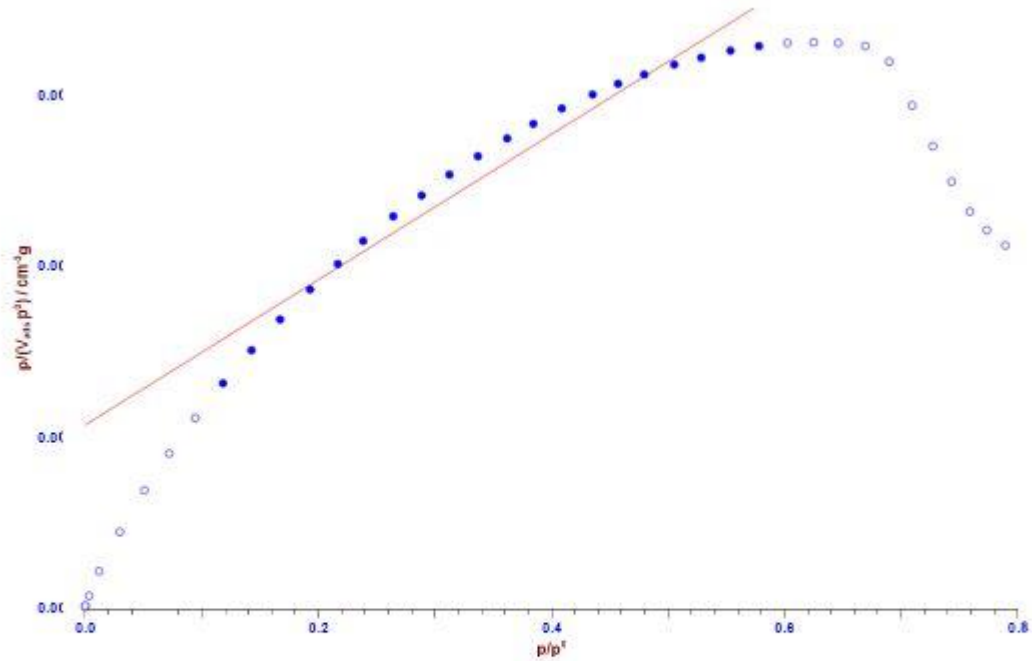

Linear regression from p/p^0 0.1 to 0.6

Offset: 0.00106888 ± 8.14315E-5

Slope: 0.00424782 ± 0.00021695

R: 0.97731935

Monoloayer volume 235.41 cm^3g^{-1}

Monoloayer amount: 10.503 mmol g^{-1}

B: 3.9741

Calculation with a molecular area of 16.2 $Å^2$

Surface area was: 1024.7 m^2g^{-1}

Mesopores (B.J.H.)

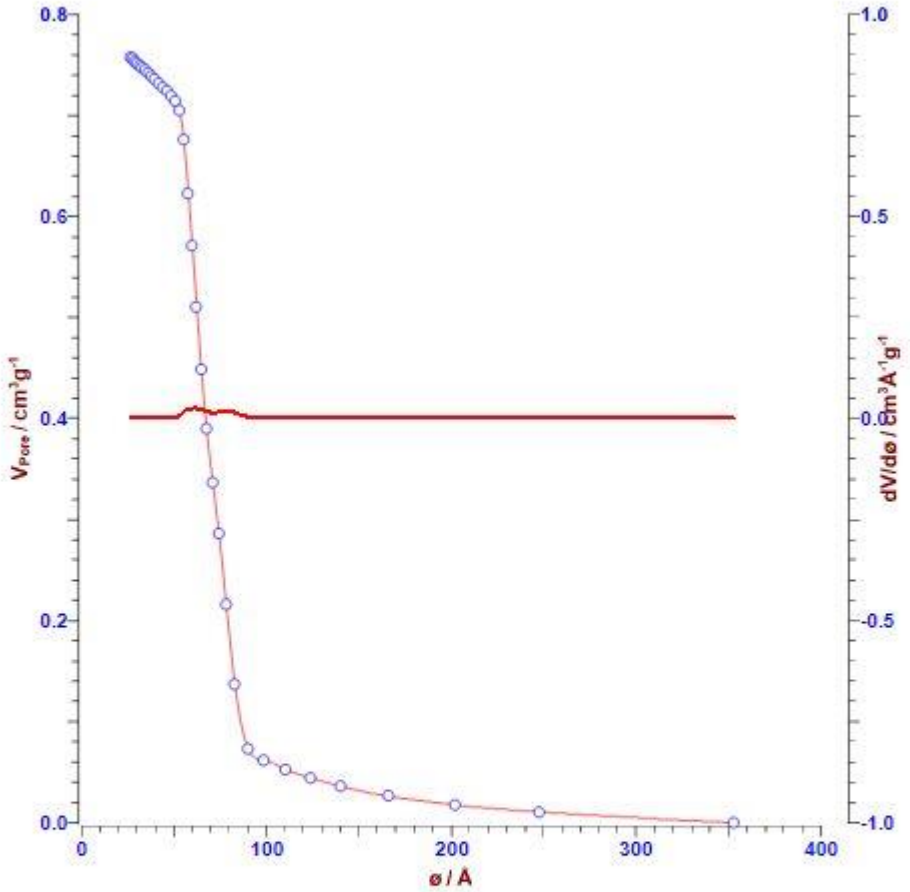

Calculations used Desorption Branch from p/p^0 0.3 to 0.95
with standard isotherm: Universal (Harkins,Jura)
from literature: ASTM Standards Designation: D 4641-87

Calculation with a molecular area of	16.2 Å²
molecular weight of	28.01 g/mol
liquid density of	0.8086 g cm⁻³
and surface tension of	8.85 Dyne cm⁻¹
Median pore diameter	68.005 Å
Maximum pore diameter	61.3 Å
Cumulative pore volume	0.7579 cm³g⁻¹
Cumulative pore area	447.79 m²g⁻¹